



The African Humid Period, rapid climate change events, the timing of human colonization, and megafaunal extinctions in Madagascar during the Holocene: Evidence from a 2m Anjohibe Cave stalagmite

Lixin Wang^{a,*}, George A. Brook^a, David A. Burney^b, Ny Riavo G. Voarintsoa^c, Fuyuan Liang^d, Hai Cheng^{e,f}, R. Lawrence Edwards^e

^a Department of Geography, University of Georgia, Athens, GA, 30602-2502, USA

^b National Tropical Botanical Garden, 3530 Papalina Road, Kalaheo, HI, 96741, USA

^c Department of Geology, University of Georgia, Athens, GA, 30602-2502, USA

^d Department of Geography, Western Illinois University, Macomb, IL, 61455, USA

^e Department of Earth Sciences, University of Minnesota, Minneapolis, MN, 55455, USA

^f Institute of Global Environmental Change, Xi'an Jiaotong University, Xi'an, Shaanxi, 710049, China

ARTICLE INFO

Article history:

Received 30 September 2018

Received in revised form

23 January 2019

Accepted 3 February 2019

Keywords:

Stalagmite

Paleoclimatology

Holocene

Human colonization

Megafaunal extinction

Southern hemisphere

ABSTRACT

Stalagmite data from Anjohibe Cave in northwest Madagascar suggest six distinct climate periods from 9.1 to 0.94 ka. Periods I and II (9.1–4.9 ka) were wetter and punctuated by a series of prominent droughts. Periods IV–VI (4–0.94 ka) were much drier and less variable. Period III (4.9–4 ka) marks the transition between wetter and drier conditions and consists of two significant droughts: the first (4.8–4.6 ka) coincides approximately with the end of the African Humid Period and the second (4.3–4.0 ka) may be the expression of the Northern Hemisphere 4.2 ka dry event in northwest Madagascar. Strong positive correlations between $\delta^{13}\text{C}$ and $\delta^{18}\text{O}$ values in Periods I–IV ($r = 0.63$ – 0.91) suggest that both isotopes were influenced by natural climate changes indicating that humans may not have been present in the area. In contrast, during Periods V ($r = 0.07$) and VI ($r = -0.12$) the “decoupling” of $\delta^{13}\text{C}$ and $\delta^{18}\text{O}$ might signal an impact from human activities starting around 2.5 ka. Rapid changes in climate during the early and middle Holocene, with prominent droughts lasting up to 800 years, did not kill off Madagascar’s megafauna, and neither did a human population, present since the early Holocene if evidence from south Madagascar is reliable. However, many extinctions occurred under the more stable climatic conditions of the late Holocene, despite an antiphase climate relationship between northern and southcentral Madagascar. This suggests that initial human colonization, or significant increase in human population, triggered the megafaunal extinctions by hunting and destruction of megafaunal habitats.

© 2019 Elsevier Ltd. All rights reserved.

1. Introduction

There is increasing evidence for abrupt global or at least hemispheric climate fluctuations at decadal to century timescales during the Holocene (Overpeck, 1996) that are often referred to as rapid climate change (RCC) events (Mayewski et al., 2004). In the Northern Hemisphere, the most significant of these events center on prolonged episodes of aridity at ca. 8.2, 5.2 and 4.2 ka, and have been identified in ice cores, marine and lake sediments, and

speleothem records (Supplement S1). Three younger RCC events have also been recognized at 3.5–2.5, 1.2–1, and 0.6–0.15 ka (Mayewski et al., 2004). Most RCC events were originally discovered in Northern Hemisphere data and are not always present in records from the Southern Hemisphere, and when identifiable, they may not be cold, or dry events. This paper presents high-resolution (better than decadal resolution in some data series) multiproxy climate data from a ca. 2 m long stalagmite (ANJ94-5) from Anjohibe Cave in northwest Madagascar, located about 15° south of the Equator. The stalagmite was collected in 1994; twenty-nine ^{230}Th ages show that it grew between ca. 9.1 and 0.94 ka.

The high-resolution Holocene record from ANJ94-5 is an opportunity to determine how the Southern Hemisphere responded

* Corresponding author.

E-mail address: wanglx@mail.uc.edu (L. Wang).

to major Northern Hemisphere climate events. In addition, as more high resolution records have become available for neighboring Africa, especially eastern and southern Africa, the new record will allow a better assessment of spatial correlations between Madagascar's climate and that of the African continent during the Holocene. An obvious question will be whether the current antiphase relationship between tropical east Africa/northwest Madagascar and southeastern Africa/southcentral Madagascar (e.g., [Ropelewski and Halpert, 1987, 1989](#); [Burrough and Thomas, 2013](#)) prevailed throughout the Holocene. The ANJ94-5 record can possibly also shed light on a vexing problem in the paleoecological history of Madagascar, namely when did humans arrive on the island and did they cause the extinction of the island's megafauna? Madagascar was once occupied by a diverse megafauna that included giant tortoises, elephant birds, pygmy hippopotami, and giant lemurs, all of which became extinct over the last 2.5 kyr ([Burney et al., 2004](#); [Crowley, 2010](#)). Early research showed that these extinctions occurred shortly after humans were thought to have arrived on the island around 2.5 ka ([Burney et al., 2003, 2004](#); [Crowley, 2010](#)). However, more recent evidence suggests human presence much earlier, even as early as 10.6 ka ([Gommery et al., 2011](#); [Dewar et al., 2013](#); [Hansford et al., 2018](#)). This new information questions not only when humans arrived but whether they were indeed responsible for the Late Holocene megafaunal extinctions. In addition, the current lack of high-resolution climate data has hampered efforts to separate human versus climatic roles in the megafaunal extinctions.

Using multiproxy climate records (carbon and oxygen stable isotopes, mineralogy, layer-specific width, growth rate, gray-scale, luminescence, and layer-bounding surfaces) from Stalagmite ANJ94-5, with a focus on variations in carbon and oxygen isotope values, this paper will address three principal questions: i) Are Northern Hemisphere Holocene RCC events apparent in the Southern Hemisphere northwest Madagascar ANJ94-5 stalagmite record; ii) How do the changes in northwest Madagascar relate to changes in areas of the adjacent African continent; and iii) Was it human activities, or were natural climate changes in any way responsible for megafaunal extinctions in Madagascar?

2. Climate of Madagascar

The climate of Madagascar is influenced by the Southeast Trade Winds from the subtropical south Indian Anticyclone, seasonal migrations of the Intertropical Convergence Zone (ITCZ), and the island's topography ([Gasse and Van Campo, 1998](#)). The mountains on the eastern side of the island cause warm and moist air from the Indian Ocean to rise, producing abundant and persistent year-round rainfall (e.g., mean annual rainfall at Toamasina is 3,368 mm; [Supplement S3](#)). Rainfall decreases westward in the rain shadow of the mountains. The arid west of the island receives seasonal rainfall during the austral summer when the ITCZ moves south and lies across the northern part of the island ([Fig. 1](#)). The northwest monsoon and strong convection usually bring heavy rains to the northwest. Tropical cyclones originating in the Indian Ocean may pass along the east coast and sometimes over northern Madagascar and head southward through the Mozambique Channel where they may be further fueled by the warm ocean waters ([Tadross et al., 2008](#)). Therefore, rainfall varies greatly across the island with the southeast being the wettest (annual rainfall >3500 mm) and the southwest the driest ([Ingram and Dawson, 2005](#)) ([Supplement S3](#)).

At inter-annual scale, Madagascar's climate is affected by variations in the Indian Ocean Dipole (IOD) and El Niño (EN)/La Niña (LN) events ([Jury, 2003](#)), which also influence rainfall in neighboring equatorial east Africa and southeast Africa. [Ropelewski and](#)

[Halpert \(1987, 1989\)](#) have shown that during EN events equatorial east Africa receives more rain while southeast Africa and south-central Madagascar receive less rain, while the opposite occurs during LN events (see also [Reason and Rouault, 2002](#); [Jury, 2003](#); [Zinke et al., 2004](#); [Ingram and Dawson, 2005](#); [Kreppel et al., 2014](#)). The rainfall dipole between east Africa/northwest Madagascar and southeast Africa/southcentral Madagascar has been confirmed by instrumental data (e.g., [Jury et al., 1995](#); [Mason and Jury, 1997](#); [Mason, 2001](#); [FEWS NET, 2014](#); [Neukom et al., 2014](#); [Zhang et al., 2015](#)).

3. Anjohibe Cave

Anjohibe Cave (15° 32' 33.3" S, 46° 53' 7.4" E) is in the Mahajanga II district of the Boeny Region of northwest Madagascar, and is ca. 73 km northeast of Madagascar's second largest city Mahajanga ([Voarintsoa et al., 2017a, b](#)). The cave lies in Tertiary limestone in the northwest ([Middleton and Middleton, 2002](#)). In Malagasy, *anjohibe* means "big cave". It has 5.3 km of passages and 14 entrances, and many rooms are more than 20 m in diameter ([Fig. 1B](#)). A large doline near the main entrance of the cave, formed by roof collapse, was a natural trap for animals in the past, which may explain the presence of fossils of extinct animals, including giant lemurs and pygmy hippopotami in some passages (e.g., [Burney et al., 1997](#)).

The area near the cave has a Köppen-Geiger Aw or Tropical wet savanna climate. Annual rainfall and temperature at Mahajanga are 1,496 mm and 27 °C, respectively ([Fig. 1, Supplement S3](#)). Rainfall is strongly seasonal; 72% falls from Dec–Feb and 93% from Nov–Mar. The warmest month is April (28.2 °C) and the coldest July (25 °C). Vegetation in the region includes dry deciduous woodland with grasses and trees that are adapted to the long dry season ([Brook et al., 1999](#); [Burgess et al., 2004](#); [Voarintsoa et al., 2017a, b](#)). The current landscape near the cave is savanna dominated by satra palms (*Bismarckia nobilis*).

There are numerous speleothems in Anjohibe Cave dating back to at least MIS 5 ([Burney et al., 1997](#); [Brook](#), unpublished ages). Stalagmite ANJ94-5 (herein referred to as ANJ94-5) grew east of the edge of the large doline formed by collapse of the cave roof ([Fig. 1](#)), and was resting on the cave floor in three sections (labeled as A, B, C in [Fig. 2a](#)) when collected.

4. Methods

The three sections of ANJ94-5 were cut in half along the growth axis and one cut surface was polished and scanned at 600-dpi resolution to obtain a reflectance image, and then exposed to UV light in a darkroom to obtain a luminescence image. Variations in reflectance and luminescence along the growth axis were derived from the scanned and photographic images using ERDAS. Powder samples for dating and stable isotope analysis were drilled from the other half of the stalagmite and slabs were cut for thin section preparation. Layer-specific width (LSW), or the width at the top of the stalagmite when a particular layer was deposited (see [Fig. 2](#) of [Sletten et al., 2013](#)), was measured at 113 locations. Mineralogical and petrographic features such as crystal structures and layer-bounding surfaces ([Railsback et al., 2013](#)) were identified in thin section. X-ray diffraction (XRD) was used to differentiate calcite and aragonite and to perform trace element analysis to characterize each mineral for selected powdered isotope samples. Twenty-nine samples of ~100 mg were drilled for ²³⁰Th dating at the University of Minnesota Isotope Laboratory using inductively coupled plasma mass spectrometry (ICP-MS), and 355 samples were drilled along the stalagmite growth axis for isotope analysis, including 47 duplicates. Isotope values are reported in ‰ relative to Vienna Pee Dee

Belemnite (VPDB). Values for aragonite were adjusted for comparison with calcite values by subtracting 1.7‰ from $\delta^{13}\text{C}$ values (Romanek et al., 1992) and 0.8‰ from $\delta^{18}\text{O}$ values (Kim et al., 2007) to account for aragonite's different fractionation of heavier isotopes. More detail on methods is given in Supplement S4.

5. Results

5.1. Morphology

The basal 30 cm of ANJ94-5 is ca. 20 cm wide but this decreases gradually to ca. 10 cm in the middle section of the stalagmite, then to ca. 7 cm in the top 40 cm, and finally to only 2.5 cm in the top 4 cm (Fig. 2b). The drip point changes at ca. 165, 90, and 40 cm from the top, and this is often accompanied by a change in stalagmite diameter (Fig. 2). LSW of 113 stalagmite layers varies from 2.0 to 9.5 cm, and averages 6 cm; the widest layers (>8 cm) are in section C of the stalagmite at 165–186 cm (Fig. 2b). Reflectance and luminescence intensity vary more or less in parallel along the growth axis, with very low values in the top 4 cm and at two Type E surfaces (158 cm and 164 cm); significantly, both values increased abruptly at ca 110–115 cm from the top (Fig. 2 c, d).

5.2. Trace elements

Only 8 of 20 elements examined in the chemical analysis were present in measurable amounts (Supplement S5). Mg in the three calcite samples ranged from 0.87 to 1.26 wt %, much higher than in the two aragonite samples. Concentrations of the other six elements were very low for all samples (less than 0.16 wt %) and were not significantly different in aragonite or calcite, except for Sr, which was more abundant in the two aragonite samples.

5.3. Mineralogy and petrography

The upper 54 cm of the stalagmite, or most of section A, is entirely aragonite at the growth axis. From 54 to 113 cm (most of section B) it alternates between calcite and aragonite, and from 113 to 197 cm (most of section C) calcite dominates (Fig. 2e). At some locations, and particularly in section B, calcite at the growth axis grades into aragonite on the stalagmite flanks. Under the microscope, calcite crystals have a columnar and palisade form (Fig. 3a and b), while aragonite crystals form elongated needle structures (Fig. 3c and d). Aragonite on the flanks of the stalagmite has needles that tend to cluster into botryoids. Calcite has less Sr and more Mg than aragonite, suggesting that all forms of calcite are primary and not formed by recrystallization from aragonite (Supplement S5).

Large-scale Type L and Type E surfaces (Railsback et al., 2013) are apparent in ANJ94-5 (Fig. 4). Below the Type L surfaces the carbonate layers are aragonite and they thin upward and LSW decreases (Figs. 2 and 6). Carbonate above these surfaces is sometimes aragonite and sometimes calcite (e.g., aragonite occurs above the Type L surface at 52 cm). Below Type E surfaces the layers are eroded or truncated particularly near the crest of the stalagmite. Prominent Type E surfaces, underlain and overlain by calcite, are apparent at 84 cm, 158 cm and 164 cm (Figs. 2 and 6).

5.4. Chronology and growth rates

Details of the 29 ICP-MS ^{230}Th ages are given in Table 1. Age uncertainties ranged from 0.54% to 3.67% with larger values generally related to low ^{238}U concentrations, low $^{230}\text{Th}/^{232}\text{Th}$ ratios, and high ^{232}Th concentrations. Very low growth rates between dated samples at ca. 52 and 90 cm are associated with Type L surfaces and at 164 cm with a Type E surface (Fig. 5).

StalAge (Scholz and Hoffmann, 2011) was used to develop an age-depth model, which shows that ANJ94-5 grew between 9.11 and 0.94 ka and that there were three hiatuses (Fig. 5). Hiatus 3 is associated with a Type E surface, where erosion at ca. 8.22 ka appears to have removed about 260 years of deposit (8.22–8.48 ka). Hiatuses 1 and 2 are at Type L surfaces and there appears to have been no deposition for about 200 years (4.19–3.99 ka) and for about 830 years (6.81–5.98 ka), respectively. Stalagmite growth was rapid between 9.11 and 7.0 ka (0.47 mm/yr), peaking between 8.21 and 8.1 ka at 0.72 mm/yr; growth was much slower after 6.0 ka (0.18 mm/yr) and slowest (0.11 mm/yr) during the last 1 kyr of growth (Figs. 5 and 6g). Growth rates were typically high immediately after a hiatus and then declined rapidly before leveling off at a slower rate, but after the longest hiatus (Hiatus 2) growth rates never reached pre-hiatus levels.

5.5. Stable isotopes

After adjusting the aragonite isotope data as outlined in Section 4, $\delta^{18}\text{O}$ values of the 308 samples range from -7.82 to -2.35 ‰ VPDB and $\delta^{13}\text{C}$ values from -13.02 to -1.47 ‰ VPDB. Based on the StalAge model, temporal resolution of individual isotope values ranges from 1 to 90 years and averages 22 years. As shown in Figs. 2 and 6, the $\delta^{18}\text{O}$ and $\delta^{13}\text{C}$ records are generally parallel except in the top 4.5 cm where $\delta^{13}\text{C}$ increases rapidly from -7.50 ‰ to -1.47 ‰ while $\delta^{18}\text{O}$ values remain fairly constant. Overall, the $\delta^{18}\text{O}$ and $\delta^{13}\text{C}$ values are significantly and positively correlated ($r = 0.85$) but for the top 4.5 cm, the correlation becomes negative ($r = -0.39$). Correlation between $\delta^{18}\text{O}$ and $\delta^{13}\text{C}$ changes in different climate periods (Section 7) and the coefficients are provided in Table 2.

In general, values of $\delta^{18}\text{O}$ and $\delta^{13}\text{C}$ are lower and more variable between 9.1 and 4.0 ka ($n = 190$) than after 4.0 ka ($n = 118$) ($\delta^{18}\text{O}$ mean -5.66 ‰ vs. -4.11 ‰, standard deviation 1.11‰ vs. 0.50‰; $\delta^{13}\text{C}$ mean -9.64 ‰ vs. -7.03 ‰, standard deviation 1.81‰ vs. 1.32‰). There are multiple abrupt, pronounced peaks in $\delta^{18}\text{O}$ and $\delta^{13}\text{C}$ at 7.4–7.3, ca. 6.8 (precedes Hiatus 2), 4.8–4.55, and 4.3–4.2 ka (precedes Hiatus 1), with the magnitude of changes greater for $\delta^{13}\text{C}$.

6. Interpretation of the proxy climate data

A detailed description of the stalagmite proxies used in this research and how variations in these proxies are interpreted in terms of climate/environmental change is provided in Supplement S6, so only a brief summary is presented here. Supplement S6 also provides a discussion of the role of kinetic processes in influencing stable isotope variations, particularly with emphasis on evaporation, and also CO_2 degassing of stalagmite dripwaters. Higher $\delta^{18}\text{O}$ and $\delta^{13}\text{C}$ values (e.g., McDermott, 2004; Fairchild et al., 2006; Lachniet, 2009) for ANJ94-5 carbonate, reduced LSW (e.g., Voarintsoa et al., 2017a), the presence of Type L surfaces (Railsback et al., 2013), and deposition of aragonite rather than calcite (e.g., Railsback et al. 1999), are together considered to be strong evidence of drier conditions. In addition, decreases in growth rate, gray-scale, and luminescence (e.g., Webster et al., 2007) suggest drier conditions based on their close correlation with other proxies. In contrast, lower $\delta^{18}\text{O}$ and $\delta^{13}\text{C}$ values, increases in LSW, the presence of Type E surfaces, deposition of calcite, and increases in growth rate, gray-scale, and luminescence suggest wetter conditions. Overall, the seven proxy time series from ANJ94-5 agree well with each other (Fig. 6) and therefore provide consistent and strong evidence of climate variations in northwest Madagascar through the Holocene.

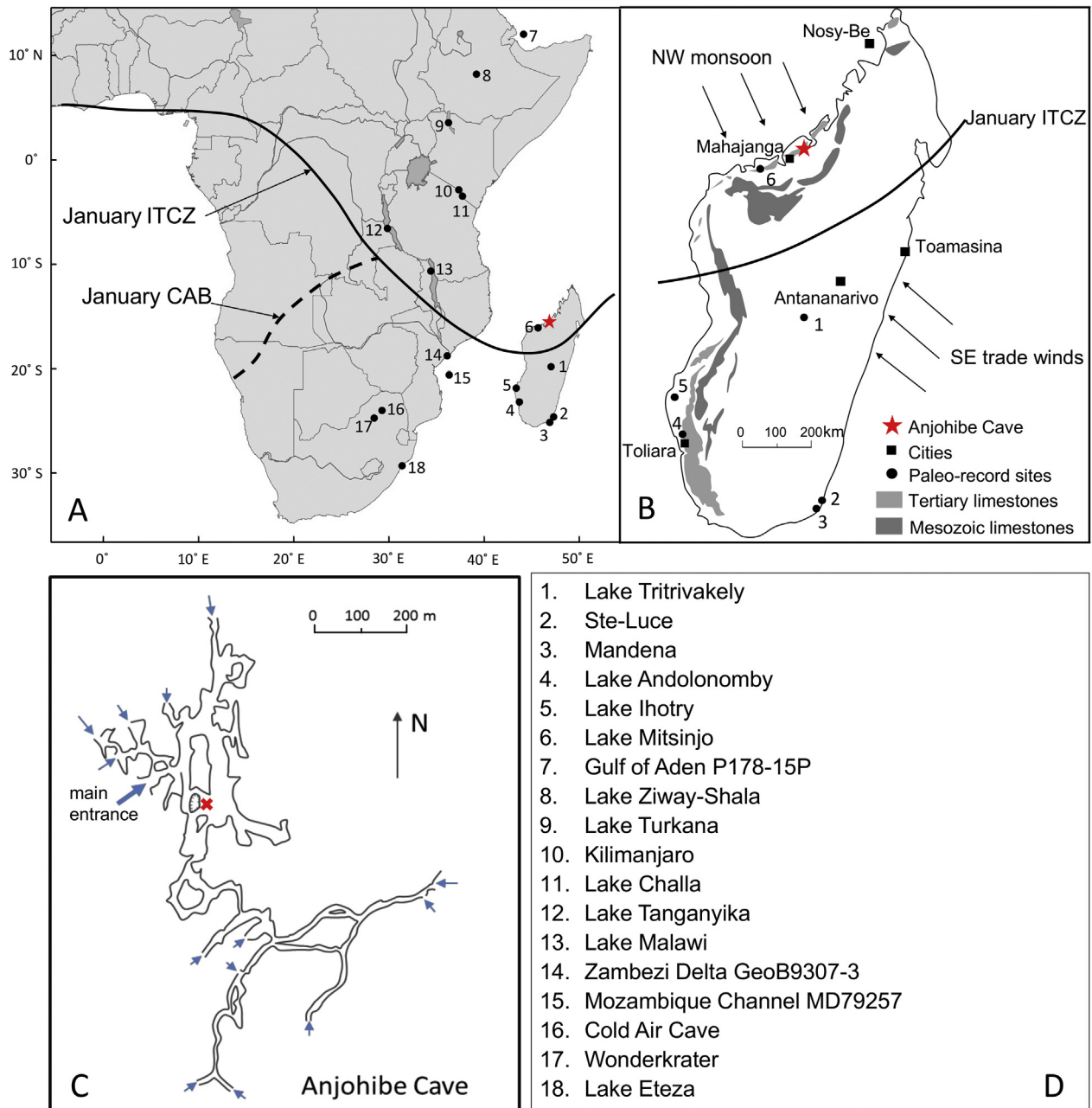


Fig. 1. Maps showing the location of Anjohibe Cave in Madagascar, and other sites mentioned in the text. (A) Site locations relative to the January positions of the ITCZ and CAB; (B) Limestone outcrops after Middleton and Middleton (2002), the position of the ITCZ across northern Madagascar in January, and the important winds affecting Madagascar; (C) Map of Anjohibe Cave (after Burney et al., 1997) showing the location of Stalagmite ANJ94-5 (red cross) and the multiple cave entrances (arrows); (D) List of numbered sites shown in (A) and (B). Details of Sites 1–18 in (D) and the proxy climate data they have provided are given in *Supplement S2*. (For interpretation of the references to color in this figure legend, the reader is referred to the Web version of this article.)

7. The ANJ94-5 record and a Holocene paleoenvironmental history for northwest Madagascar

Six distinct climate periods, Periods I to VI, are apparent in the ANJ94-5 climate proxy data based on differences in mean isotope values, isotope variability, and degree of correlation between $\delta^{18}\text{O}$ and $\delta^{13}\text{C}$ (Fig. 6, Table 2). Period I is similar to the “Malagasy early Holocene interval” of Voarintsoa et al. (2017b) which lasted from ca. 9.8–7.8 ka BP (Fig. 7), while Periods II–V are approximately equivalent to their “Malagasy mid-Holocene interval” (ca. 7.8–1.6 ka BP), and Period VI is the first part of their “Malagasy late Holocene interval” (ca. 1.6–0 ka BP). Because the ANJ94-5 record ends at 0.94 ka,

we used published data for the 0.94–0 ka period from other Anjohibe Cave stalagmites (AB2, ANJB-2, and MA3; Burns et al., 2016; Scroxton et al., 2017; Voarintsoa et al., 2017a, b) and Stalagmite MAJ-5 from Anjokipoty Cave (ca. 16.5 km southwest of Anjohibe Cave, Voarintsoa et al., 2017b) to extend our discussion of Holocene climates in northwest Madagascar to the present (Fig. 7). In June 2018, the International Union of Geological Sciences ratified the proposal by the International Subcommission on Quaternary Stratigraphy (ISQS) to subdivide the Holocene Series/Epoch into three stages: the Greenlandian (11.7–8.326 ka), Northgrippian (8.326–4.25 ka), and the Meghalayan (4.25 ka –1950 CE) (<http://www.stratigraphy.org/index.php/ics-chart-timescale>). As will be

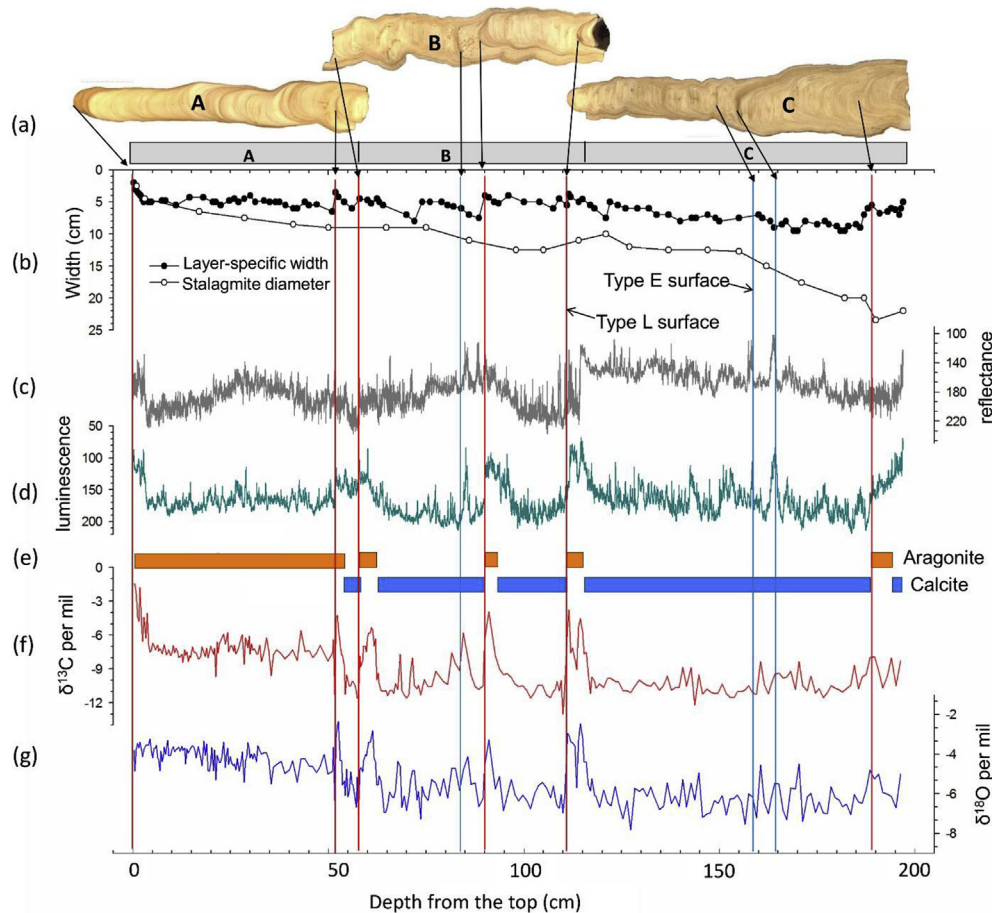


Fig. 2. Variations in climate proxy data along the growth axis of ANJ94-5. (a) Stalagmite sections A, B, and C; (b) stalagmite diameter and LSW; (c) reflectance; (d) luminescence; (e) mineralogy; (f) $\delta^{13}\text{C}$; (g) $\delta^{18}\text{O}$. The vertical red lines show major Type L surfaces and the blue lines major Type E surfaces. Higher values of reflectance indicate whiter carbonate with less detritus; higher values of luminescence indicate higher levels of organic acids. (For interpretation of the references to color in this figure legend, the reader is referred to the Web version of this article.)

seen below, the stage boundaries in the new system are similar but not the same as the climate boundaries we identify in the ANJ94-5 record.

Period I: 9.1–7.5 ka. The mineralogy is calcite except for a basal section of aragonite deposited over the first ca. 200 years of the record. Mean values of $\delta^{18}\text{O}$ and $\delta^{13}\text{C}$ are the lowest of the entire record with moderate variability (Table 2). Growth rates are high reaching a maximum around 8.2 ka. Reflectance and luminescence are also uniformly high except for the first ca. 200 years. LSWs are relatively low in the basal aragonite but increase sharply in the calcite, reaching a maximum at ca. 8.8 ka and then decreasing steadily to 7.5 ka. A Type E surface at ca. 8.2 ka, formed by input of undersaturated drip water that removed ca. 260 years of previously deposited carbonate (Hiatus 3 from 8.22 to 8.48 ka at 164 cm depth), records a time of significantly increased and possibly more intense rainfall. Together, the multiproxy climate data suggest that conditions were wet during this period, and in fact much wetter than any period afterwards. The aragonite deposits, low LSWs, and low luminescence and reflectance of the first 200 years, suggest that conditions during the initial deposition of ANJ94-5 were slightly drier than the overall wetness of the period, but still wetter than later periods. The $\delta^{13}\text{C}$ values (mean -10.29‰) point to a predominantly C_3 vegetation, most likely trees.

Data from Stalagmite ANJB-2 for 9–7.8 ka (Voarintsoa et al., 2017b) cover much of Period I and parallel the ANJ94-5 data. Values of $\delta^{18}\text{O}$ and $\delta^{13}\text{C}$ from both stalagmites are strongly and

positively correlated ($r = 0.67$ for ANJ94-5, $r = 0.72$ for ANJB-2) suggesting that natural conditions are affecting rainfall and vegetation in the area. Both stalagmites show wetter conditions centered at ca. 8.8 ka, and pronounced wet conditions at 8.2 ka. The interval from 8.7 to 8.3 ka was dry, as suggested by ANJB-2, while in ANJ94-5 much of the interval was removed by erosion at 8.2 ka. The pronounced wet interval at ca. 8.2 ka correlates in time with the 8.2 ka event of the Northern Hemisphere, where it is typically associated with cold, dry conditions at high latitudes and a brief cool and dry/windy period at low latitudes (Supplement S1). However, low $\delta^{13}\text{C}$ and $\delta^{18}\text{O}$ values, low reflectance and luminescence values, and the presence of Type E surface at ca. 8.2 ka in Stalagmite ANJ94-5, and low $\delta^{13}\text{C}$ and $\delta^{18}\text{O}$ values in Stalagmite ANJB-2 (Voarintsoa et al., 2017b), all suggest wetter, not drier, conditions in north-west Madagascar (Voarintsoa et al., 2019). Cheng et al. (2009) compared stalagmite records from China, Oman and Brazil, looking for evidence of the 8.2 ka event and found that while China and Oman experienced drought, Brazil was much wetter. All these suggest that during the 8.2 ka event, low-latitude areas were not uniformly dry. Instead, the two hemispheres show an opposite moisture pattern, with wetter conditions in southern low latitudes and drier conditions in northern low latitudes. This moisture pattern was attributed to a southward shift of the ITCZ due to cooling at high latitudes of the Northern Hemisphere (Cheng et al., 2009), which brings increased rainfall to southern low latitudes.

Period II: 7.5–4.9 ka. The mineralogy is still dominated by calcite

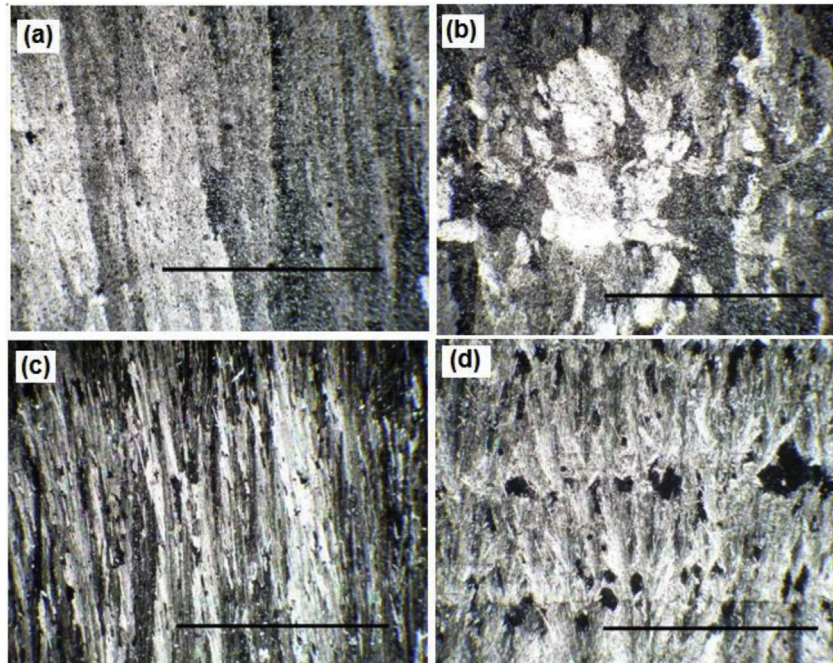


Fig. 3. Photomicrographs showing typical calcite and aragonite fabrics in ANJ94-5. The scale bar is 1 mm. (a) calcite with palisade structure at 85 cm; (b) calcite with columnar structure at 110 cm; (c) aragonite with long needle crystals at 12 cm; (d) aragonite with a shorter and coarser fabric at 2 cm.

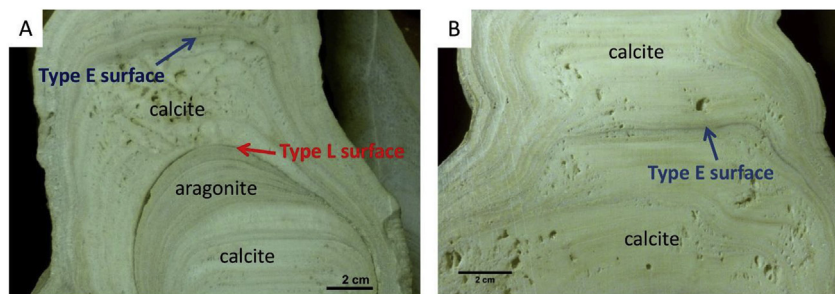


Fig. 4. Representative layer-bounding surfaces and mineralogy in ANJ94-5. (A) Type L surface at 90 cm, which is followed by a major hiatus in stalagmite growth, and a Type E surface at 84 cm, which is rich in dark detrital material. (B) Type E surface at 164 cm visible as a dark line.

but with four distinct aragonite zones varying from ca. 150–250 years of aragonite deposition (Fig. 6). Values of $\delta^{18}\text{O}$ and $\delta^{13}\text{C}$ are strongly and positively correlated ($r = 0.86$), and variability is much higher than in the previous period (Table 2). Mean $\delta^{13}\text{C}$ and $\delta^{18}\text{O}$ values are slightly higher than during Period I but the baseline low values (ca. -11‰ and -6.5‰ for $\delta^{13}\text{C}$ and $\delta^{18}\text{O}$, respectively) are similar between the two periods. Luminescence and reflectance are lower during dry intervals, particularly early in the period. However, from 6 to 4.9 ka, when calcite was deposited, luminescence decreased steadily while reflectance increased. The stalagmite grew rapidly at a similar rate to that of Period I prior to Hiatus 2. Growth was much slower after 6.0 ka, reaching its lowest level around 5.4 ka. Overall, the multiproxy records suggest greater climate variability than during Period I. Although the wet intervals compare with conditions in Period I, Period II is punctuated by a series of much drier intervals, often associated with aragonite deposition and Type L surfaces. Most prominent is Hiatus 2 from 6.81 to 5.98 ka at 90 cm depth, when conditions were dry enough to halt stalagmite deposition for a period of 830 years. In addition, there were other droughts centered at 7.4, 6.9, 5.9, 5.4, and 5.1 ka, each lasting ca. 100–300 years with $\delta^{18}\text{O}$ and $\delta^{13}\text{C}$ values increasing

by up to ca. 3.5‰ and 6.5‰ , respectively. These rapid climate change events began and ended abruptly, sometimes within a decade. It is possible that the less prominent droughts at ca. 5.4 and 5.2 ka together represent the expression in northwest Madagascar of the global 5.2 ka RCC event (Supplement S1). The frequent and long-lasting droughts during this period might explain hiatuses in many stalagmites at Anjohibe (ANJB-2) and Anjokipoty Cave (MAJ-5). During Period II, $\delta^{13}\text{C}$ values range from -13.02‰ to -3.77‰ , and vary significantly with changes in climate suggested by $\delta^{18}\text{O}$ values. This implies that vegetation responded to natural changes in climate. Trees dominated during wetter intervals but C_4 grasses increased during drier intervals and became abundant during major droughts.

Period III: 4.9–4 ka. This period is dominated by two dry intervals when aragonite was deposited that are separated by a wetter interval of calcite deposition. The first dry interval was between 4.8 and 4.6 ka, centered at ca. 4.7 ka. The second dry interval starts around 4.3 ka and includes a hiatus of ca. 200 years from 4.2 to 4 ka (Hiatus 1 at 51.9 cm depth). Values of $\delta^{13}\text{C}$ and $\delta^{18}\text{O}$ are highly correlated ($r = 0.91$) and have the highest variability among the six periods (Table 2). Average growth rate was 0.16 mm/yr, and

Table 1
Stalagmite ANJ94-5 ²³⁰Th age data.

Sample ID	Depth (cm)	²³⁸ U (ppb)	²³² Th (ppt)	²³⁰ Th / ²³² Th (atomic x10 ⁶)	δ ²³⁴ U (measured) ^a	²³⁰ Th / ²³⁸ U (activity)	²³⁰ Th Age (uncorrected)	²³⁰ Th Age (corrected) ^b	δ ²³⁴ U _{initial} (corrected) ^c	²³⁰ Th Age (Year BP) (corrected) ^d
ANJ94-5-U010	0.3	1098.9±1.6	392±8	507±13	5±1.4	0.011±0.0001	1197±16	1187±17	5±1	1122±17
ANJ94-5-W1	1	701.5±2.5	762±15	154±4	9.6±2.8	0.0102±0.0002	1103±18	1071±28	9.6±2.8	1009±28
ANJ94-5-U050	2.2	1766.4±4.3	5134±104	68±1	4.7±9	0.0119±0.0001	1301±12	1217±61	5±2	1152±61
ANJ94-5-U078	3.1	1600.9±3.0	731±15	432±10	3.8±1.6	0.012±0.0001	1308±11	1295±15	4±2	1230±15
ANJ94-5-W2	3.5	602.9±2.1	469±10	268±7	7.0±2.8	0.0126±0.0002	1375±25	1352±30	7.0±2.8	1290±30
ANJ94-5-U090	3.75	2146±3.3	581±12	747±17	2.7±1.4	0.0123±0.0001	1341±11	1333±12	2.7±1.4	1268±12
ANJ94-5-U110	4.4	1666±3.0	392±8	887±19	5.1±1.4	0.0127±0.0001	1382±9	1375±10	5±1	1310±10
ANJ94-5-U120	5	1980.8±3.9	785±16	543±11	3.0±1.5	0.0130±0.0001	1428±8	1416±11	3±1	1351±11
ANJ94-5-T4	13.5	569.4±1.4	155±3	1255±31	50.8±2.6	0.0207±0.0003	2170±27	2162±27	51±3	2104±27
ANJ94-5-T3	25	637.4±2.0	796±4	375±5	82.6±3.0	0.0284±0.0004	2897±37	2864±41	83±3	2806±41
ANJ94-5-T2	32.7	596.6±2.3	484±4	709±15	83.2±3.9	0.0349±0.0007	3567±37	3545±37	84±4	3487±37
ANJ94-5-T1	41.2	723.9±2.2	87±4	5260±226	86.1±3.0	0.0382±0.0004	3902±39	3899±39	87±3	3841±39
ANJ94-5-W3	51	340.5±1.1	187±4	1096±30	3.2±2.6	0.0366±0.0005	4047±	4031±56	3.2±2.6	3969±56
ANJ94-5-51.7	51.7	123.5±0.1	217±5	349±10	5.3±1.5	0.0372±0.0007	4113±78	4063±86	5.4±1.5	3996±86
ANJ94-5-W4	53.5	667.7±2.1	200±4	2192±48	5.0±2.5	0.0398±0.0002	4407±29	4398±30	5.0±2.6	4336±30
ANJ94-5-W5	61.5	789.5±2.5	278±6	2028±43	2.5±2.5	0.0433±0.0002	4810±27	4800±27	2.5±2.5	4738±27
ANJ94-5-M5	69.7	84.2±0.2	25±4	2874±417	82.6±5.4	0.0522±0.0010	5383±106	5375±106	84±5	5317±106
ANJ94-5-W6	84.5	77.1±0.3	633±13	114±3	7.6±3.2	0.0569±0.0013	6335±148	6098±224	7.8±3.2	6036±224
ANJ94-5-M4	89.2	139.6±0.3	94±13	1350±48	41.7±2.9	0.0551±0.0006	8924±73	5905±73	42±3	5847±73
ANJ94-5-M3	91.7	592.4±1.4	531±5	1154±13	11.3±2.5	0.0628±0.0004	6985±53	6959±53	11.6±2.5	6901±53
ANJ94-5-M2	109.4	69.1±0.2	73±4	1068±66	118.8±4.5	0.0685±0.0013	6880±140	6853±140	121±4.5	6795±140
ANJ94-5-M1	113.65	781±2.2	248±5	3808±81	110.6±2.9	0.0734±0.0006	7450±66	7442±66	113±3	7384±66
ANJ94-5-6B	115	1113.7±6.4	622±4	1947±18	1.7±3.8	0.0660±0.0006	7428±75	7412±75	1.8±3.8	7354±75
ANJ94-5-W7	128	890.7±3.0	489±10	2072±42	3.2±2.6	0.0690±0.0003	7776±40	7760±42	3.3±2.7	7698±42
ANJ94-5-5B	144.2	111.5±0.3	70±4	1874±107	-0.2±3.7	0.0715±0.0011	8092±132	8074±132	-0.2±3.8	8016±132
ANJ94-5-4B	163.7	92.3±0.2	33±3	3351±346	3±3.6	0.0731±0.0012	8254±147	8243±147	3.1±3.7	8185±147
ANJ94-5-3B	166	1158±3.9	287±3	5035±61	1.4±2.2	0.0756±0.0005	8564±57	8557±57	1.4±2.3	8499±57
ANJ94-5-2B	180	1374±3.8	117±4	15175±499	2.6±1.8	0.0786±0.0004	8901±51	8898±51	2.7±1.9	8840±51
ANJ94-5-1B	193.25	1234.1±3.3	268±4	6081±89	1.6±1.8	0.0801±0.0005	9086±57	9080±57	1.7±1.9	9022±57

Year of sample analysis indicated by shading: no shading = 2008; blue = 2012; green = 2015; grey = 2017. (For interpretation of the references to color in this figure legend, the reader is referred to the Web version of this article)

^a δ²³⁴U = ((²³⁴U/²³⁸U)_{activity} - 1) × 1000.

^b Corrected ²³⁰Th ages assume the initial ²³⁰Th/²³²Th atomic ratio of 4.4 ± 2.2 × 10⁻⁶. Those are the values for a material at secular equilibrium, with the bulk earth ²³²Th/²³⁸U value of 3.8. The errors are arbitrarily assumed to be 50%.

^c δ²³⁴U_{initial} was calculated based on ²³⁰Th age (T), i.e., δ²³⁴U_{initial} = δ²³⁴U_{measured} × e^{1234λT}.

^d BP stands for “Before Present” where the “Present” is defined as the year 1950 A.D.

the LSW, luminescence, and reflectance curves generally follow the isotope curves. The 4.8–4.6 ka drought is clearly defined by the rapid and significant changes in isotope values (Fig. 7). Between 4.34 and 4.2 ka, ANJ94-5 δ¹³C and δ¹⁸O values changed from -11.28‰ to -4.26‰ and -6.15‰ to -2.35‰, respectively (Supplement S7), and this was followed by a major Type I surface at 51.9 cm, and a growth hiatus of ca. 200 years from 4.2 to 4 ka. These changes indicate a major drought from 4.3 to 4 ka that may be an expression of the global 4.2 ka RCC event in northwest Madagascar, while the 4.8–4.6 ka drought may be a yet unreported global RCC event (Supplement S1). Stalagmite growth resumed at ca. 3.99 ka (3.93–4.03 ka with age errors), suggesting that after the 4.2 ka drought, climate became wet enough to trigger further growth of ANJ94-5. Based on carbonate isotope values (δ¹³C = -11.27‰, δ¹⁸O = -6.34‰), conditions were as wet as those in the interval separating the ca. 4.7 and 4.2 ka droughts. However, the wet period was brief, lasting only a decade or so, before the climate became permanently much drier in Periods IV–VI.

Period IV: 4–2.5 ka. The mineralogy is entirely aragonite. Growth was rapid during the first 200 years and then became similar to that of Period III. Luminescence, reflectance, and LSW are less variable than in previous periods. Isotope values are permanently higher and much less variable than during Periods I to III (Table 2). In fact, even the low isotope values at ca. 3.6, 3.1, and 2.6 ka are still higher than the baseline low values of the earlier periods. Overall, mean isotope values are intermediate between the lowest values in Periods I and II and peak values of Period III. In addition, values of δ¹⁸O and δ¹³C increase steadily towards 2.6 ka (Fig. 7). The multiproxy data suggest three brief (lasting 20–30 years) relatively wet intervals at ca. 3.60, 3.12, and 2.62 ka, but overall conditions were becoming drier over time. Mean δ¹³C is -7.24‰ suggesting a mixed C₃ and C₄ vegetation, perhaps satra palm savanna similar to today. Values of δ¹³C and δ¹⁸O are strongly correlated (r = 0.63) but less so than during earlier periods; nevertheless they still suggest the dominance of climate in controlling the environment at this time (Table 2). At Lake Mitsinjo,

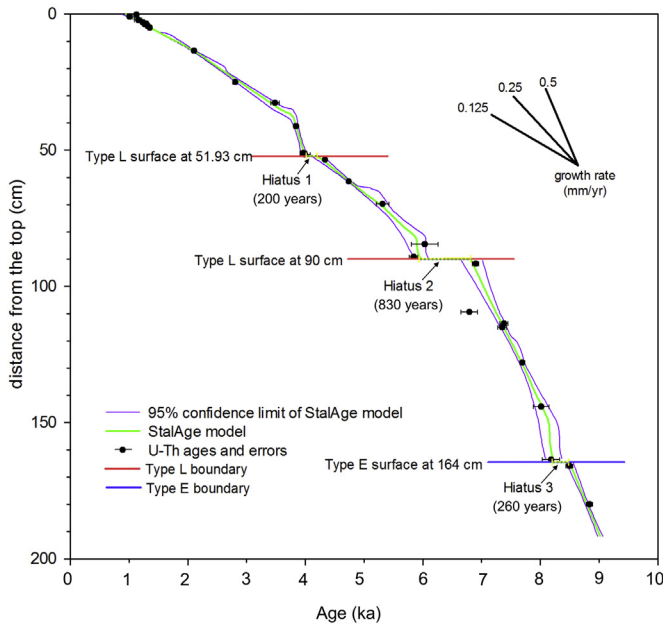


Fig. 5. Age-depth model for ANJ94-5 using the StalAge algorithm, and hiatuses associated with the major Type E and Type L surfaces.

about 115 km west-southwest of Anjohibe Cave, pollen indicates higher rainfall than today that supported a mosaic of dry forest and grassland after ca. 3.5 ka until sometime before 1.0 ka when the lake dried up (Matsumoto and Burney, 1994; Wright et al., 1996). Higher rainfall is also evident by generally lower ANJ94-5 $\delta^{18}\text{O}$ values in Period IV compared to later periods (Fig. 7).

Period V: 2.5-1.53 ka. The mineralogy is entirely aragonite. Luminescence, growth rate and LSW are similar to Period IV while reflectance is higher. The mean value of $\delta^{18}\text{O}$ is slightly higher than during Period IV but mean $\delta^{13}\text{C}$ is slightly lower and isotopic variability is the lowest of the entire series (Table 2). The multiproxy data suggest that climate was similar to or only slightly drier than Period IV, and a little less variable. However, the strong positive correlations between $\delta^{18}\text{O}$ and $\delta^{13}\text{C}$ in Periods I to IV disappeared in Period V ($r = 0.07$). The $\delta^{18}\text{O}$ values are more or less constant, whereas $\delta^{13}\text{C}$ values decrease slightly toward ca. 2.0 ka, before increasing again over the rest of the period (Fig. 7). This “decoupling” of $\delta^{13}\text{C}$ and $\delta^{18}\text{O}$ might signal an impact from human activities. Humans may have begun modifying the vegetation of the Anjohibe Cave region by 2.5 ka. Archaeological evidence suggests there was a transition from foraging to agriculture ca. 3–1.5 ka (Dewar et al., 2013). It is possible that humans altered the vegetation near Anjohibe Cave around this time perhaps by burning C_4 grasses thus increasing the contribution of C_3 tree and bush root respiration to the soil air, resulting in lower $\delta^{13}\text{C}$ values that were transferred to ANJ94-5. In addition, human activities might also

have caused soil erosion from the limestone surfaces, leaving soils only in solutionally-widened fractures (grikes) where bushes and trees would take root, also contributing to lower $\delta^{13}\text{C}$. No archaeological settlements are known near the cave but there are numerous sites about 50 km to the west-southwest between Mahajanga and Mitsinjo. All are younger than ca. 0.9 ka (Wright et al., 1996) and so provide supporting evidence for human disturbance during Periods VI and VII rather than during Period V. However, the area is not well studied so that earlier settlements may yet be discovered. Interestingly, there is evidence of cattle at the Andavambatobe karst sinkhole and cave near Lake Mitsinjo dating to around 0.55 ka (Wright et al., 1996). The streams and pools in Anjohibe Cave may also have been used by hunters and herders as a source of water, while the trees in the entrance sinkhole may have provided shade.

Period VI: 1.53-0.94 ka. The mineralogy is aragonite but crystal needles are shorter and narrower than during Periods III and IV. The growth rate was the lowest of the entire record, and LSW decreased rapidly, culminating in a prominent Type L surface at the top of the stalagmite, indicating declining drip water. For $\delta^{18}\text{O}$, the mean value (-3.80‰) is only slightly higher than that of Period V (-3.90‰) and standard deviations are similar between the two periods (Table 2). However, there appears to have been a rapid drying event at ca. 1.5 ka, as suggested by the ANJ94-5 $\delta^{18}\text{O}$ record, and three other stalagmite records for Anjohibe Cave. In ANJ94-5, $\delta^{18}\text{O}$ values increase rapidly from -6.0 to -4.1‰ ($+1.9\text{‰}$), and in Stalagmites MA3, AB2, and ANJB-2 they increase by 2.7‰ (-6.0 to -3.3‰), 1.9‰ (-6.0 to -4.1‰), and 3.9‰ (-6.2 to -2.3‰), respectively (Fig. 7). The Anjokipoty Cave MAJ-5 stalagmite record also shows evidence of dry intervals during Period VI with high $\delta^{18}\text{O}$ values of -1.9‰ and -2.7‰ at 1.55 ka and 1.09 ka, respectively, separated by a wetter interval centered on a low value of -6.7‰ at 1.29 ka. The climate drying recorded by the Anjohibe and Anjokipoty Cave stalagmites correlates with evidence from Lake Mitsinjo that the lake dried up prior to 1.0 ka probably between 1.2-1.0 ka (Matsumoto and Burney, 1994; Wright et al., 1996).

During Period VI, ANJ94-5 $\delta^{13}\text{C}$ values increased significantly from -7.5‰ at 1.307 ka to -1.47‰ at 0.985 ka, within the short span of only 322 years. This indicates either a massive shift to C_4 grasses, or a much sparser vegetation cover and less soil CO_2 , the latter also suggested by decreasing stalagmite luminescence. Values of $\delta^{18}\text{O}$ and $\delta^{13}\text{C}$ are weakly and negatively correlated ($r = -0.12$), showing a continuation of the “decoupling” that began during Period V (Tables 2 and 3). Values of $\delta^{13}\text{C}$ for Stalagmites MA3, AB2, ANJB-2 and MAJ-5 confirm the basic information from ANJ94-5 (Fig. 7). In all five records $\delta^{13}\text{C}$ values increase dramatically after ca. 1.6 ka, although the timing varies (largely due to age uncertainties), beginning at ca. 1.6 ka (MAJ-5), 1.5 ka (ANJB-2), 1.3 ka (ANJ94-5 and MA3), and 1.1 ka (AB2) in the different records (see Supplement S7 for ANJ94-5 data).

The drying of the climate at Anjohibe and Anjokipoty Cave during the early part of Period VI, indicated by increased $\delta^{18}\text{O}$ and $\delta^{13}\text{C}$ values, was likely synchronous with the major arid event that

Table 2
ANJ94-5 $\delta^{13}\text{C}$ and $\delta^{18}\text{O}$ characteristics during Periods I to VI.

Periods	Age (ka)	Depth (cm)	Number of Samples	$\delta^{13}\text{C}$ (‰ VPDB)				$\delta^{18}\text{O}$ (‰ VPDB)				Correlation $\delta^{13}\text{C}$ - $\delta^{18}\text{O}$
				min	max	mean	Standard deviation	min	max	mean	Standard deviation	
I	9.2–7.5	120–197	76	-12.19	-7.89	-10.29	0.94	-7.82	-4.49	-6.23	0.70	0.67
II	7.5–4.9	64–120	77	-13.02	-3.77	-9.56	1.95	-7.28	-2.47	-5.52	1.10	0.86
III	4.9–4	51.5–64	37	-11.58	-4.26	-8.46	2.22	-7.04	-2.35	-4.79	1.18	0.91
IV	4–2.5	19.5–51.5	61	-9.70	-5.60	-7.24	0.80	-5.52	-3.40	-4.35	0.49	0.63
V	2.5–1.53	6.9–19.5	37	-8.42	-6.85	-7.59	0.39	-4.83	-3.29	-3.90	0.36	0.07
VI	1.53–0.94	0–6.9	20	-7.50	-1.47	-5.34	2.14	-4.86	-3.23	-3.80	0.37	-0.12

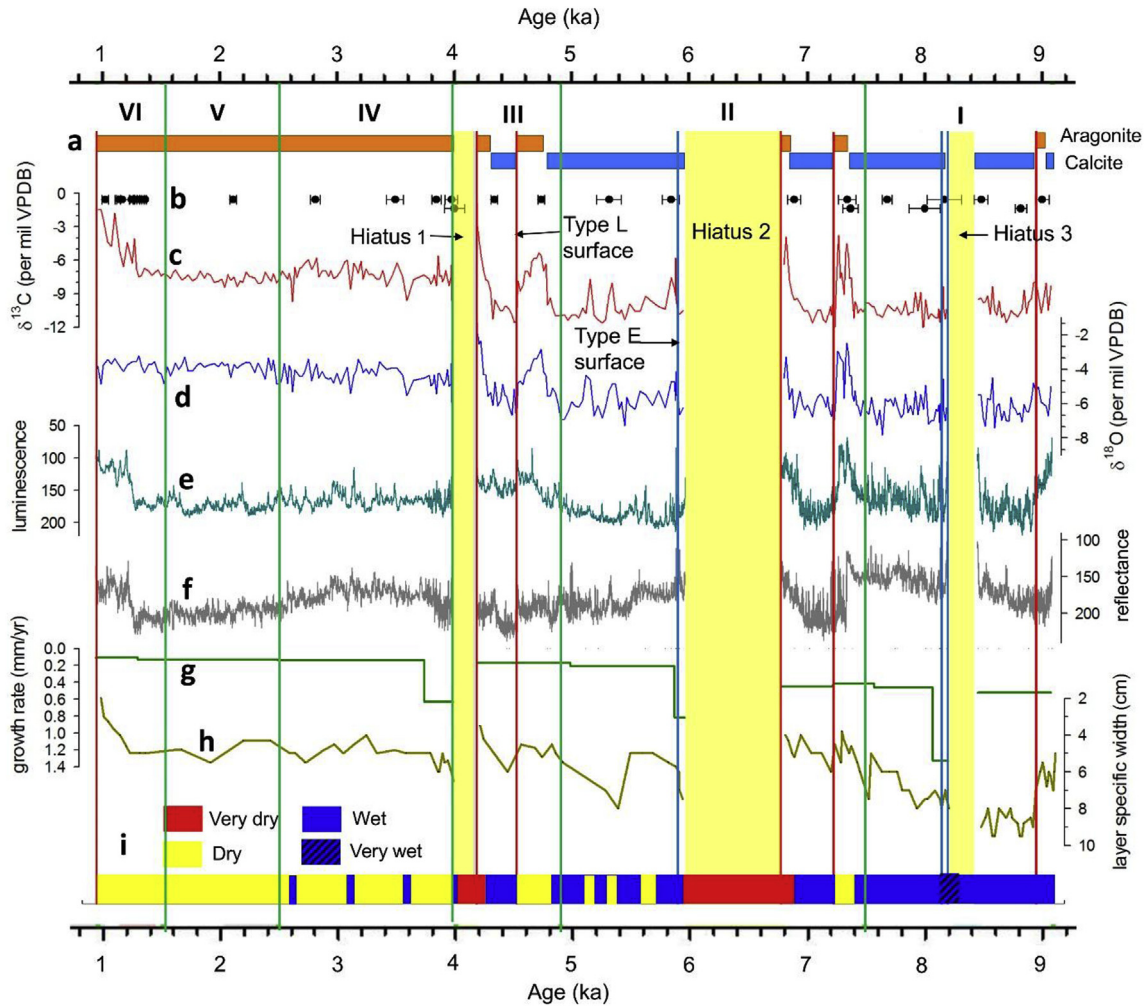


Fig. 6. Proxy evidence of climate change from ANJ94-5. (a) mineralogy; (b) ^{230}Th ages; (c) $\delta^{13}\text{C}$; (d) $\delta^{18}\text{O}$; (e) luminescence; (f) reflectance; (g) growth rate; (h) layer specific width; (i) inferred hydroclimate conditions: very wet refers to conditions that caused erosion of the stalagmite; very dry refers to conditions that were too dry for stalagmite growth. The vertical yellow bars, red lines and blue lines show hiatuses, Type L surfaces, and Type E surfaces, respectively. The green solid vertical lines separate climate Periods I-VI. (For interpretation of the references to color in this figure legend, the reader is referred to the Web version of this article.)

desiccated Lake Mitsinjo. Therefore, it is likely that the changes in stalagmite isotopes were at least partly due to a significant decrease in rainfall. However, in three of the five stalagmite records in Fig. 7, $\delta^{13}\text{C}$ and $\delta^{18}\text{O}$ values are negatively correlated ($r = -0.12$ for ANJ94-5, -0.11 for AB2, -0.07 for MA3), and in the other two they are positively but weakly correlated (0.10 for ANJB-2, 0.24 for MAJ-5; see Table 3). In a study of 128 stalagmite records, Mickler et al. (2006) found only 4% showing a negative correlation between $\delta^{18}\text{O}$ and $\delta^{13}\text{C}$ suggesting that the normal balance between climate and stalagmite isotope proxies at Anjohibe and Anjokipoty Cave might have been disturbed. Frumkin et al. (2000) invoked intense soil erosion during times of intense rainfall to explain a negative correlation in a Jerusalem stalagmite. In northwest Madagascar it is likely that a decrease in rainfall together with a major human impact on the landscape are the most likely causes of the decoupling of $\delta^{18}\text{O}$ and $\delta^{13}\text{C}$ in Periods V and VI, with the greatest impact coming in Period VI.

Period VII: 0.94–0.34 ka. Period VII is recorded in three Anjohibe Cave stalagmites (AB2, ANJB-2 and MA3) and one Anjokipoty Cave stalagmite (MAJ-5) (Burns et al., 2016, Scroxtion et al., 2017, Voarintsoa et al., 2017a, b) but only Stalagmites ANJB-2, AB-2, and MAJ-5 cover the entire period. The $\delta^{18}\text{O}$ isotope data suggest a relatively dry period overall but one wetter than Period VI,

particularly in the first ca. 295 years and the last 162 years (Fig. 7). The $\delta^{13}\text{C}$ values remain high in ANJB2 and AB2, suggesting a relatively stable vegetation consisting mainly of C_4 grasses at Anjohibe Cave. In contrast, MAJ-5 records a rapid and continuous decrease in $\delta^{13}\text{C}$ values from -2.1‰ to -7.9‰ suggesting a change back to a C_3 dominated vegetation at Anjokipoty Cave. The persistence of grass at Anjohibe Cave and the change back to C_3 bushes and trees at Anjokipoty Cave may indicate continued human disturbance at Anjohibe but a reversion to the “natural” C_3 -dominated vegetation, or simply an end to human disturbance at Anjokipoty. In addition, positive and improved correlation coefficients between $\delta^{13}\text{C}$ and $\delta^{18}\text{O}$ for stalagmites AB2 ($r = 0.45$), ANJB-2 ($r = 0.44$), and MA3 ($r = 0.60$) indicate that the vegetation was responding to natural variations in rainfall. Together, the stalagmite data support the pollen data from Lake Mitsinjo where the savanna vegetation at ca. 1.0–0.5 ka, after the desiccation event, indicate an increase in rainfall (Matsumoto and Burney, 1994).

Period VIII: 0.34–0.0 ka. Period VIII is recorded in stalagmites AB2, AB3 (not shown in Fig. 7), ANJB-2, and MAJ-5 (Burns et al., 2016; Scroxtion et al., 2017; Voarintsoa et al., 2017b). The $\delta^{18}\text{O}$ data in all four stalagmites indicate a slight increase in rainfall in northwest Madagascar, while the $\delta^{13}\text{C}$ data suggest higher soil CO_2 levels and/or more C_3 plants at Anjohibe Cave and lower soil CO_2

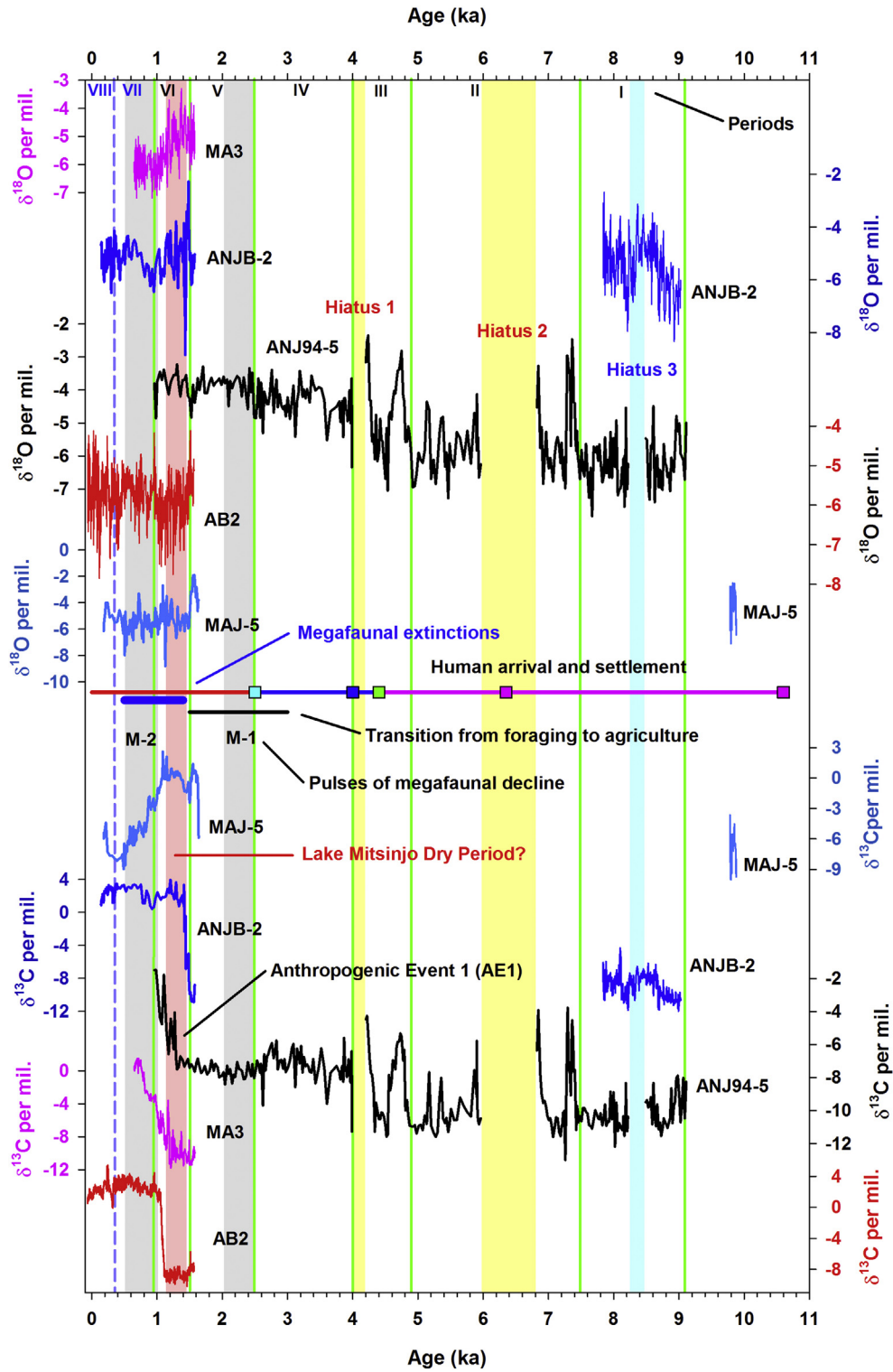


Fig. 7. Holocene isotope records from four Anjohibe Cave stalgmities (ANJ94-5, ANJB-2, AB2, and MA3) and one Anjokipoty Cave stalgmite (MAJ-5). Anjokipoty Cave is 16.5 km southwest of Anjohibe Cave. Periods I-V are based on ANJ94-5 data, and Periods VI-VIII on ANJ94-5, ANJB-2, AB2, MA3, and MAJ-5 data. Data from a fifth Anjohibe Cave stalgmite, AB3 (Burns et al., 2016), are not included as the record is almost identical to that from AB2. Dates for human arrival and settlement, the transition from foraging to agriculture, and megafaunal extinctions (summarized from Crowley, 2010; Virah-Sawmy et al., 2010; Dewar et al., 2013; and Hansford et al., 2018) are shown in the center of the figure. The cyan square shows the accepted time of human arrival of about ca. 2.5 ka as known in 2010 and is based on the age of a human-modified sloth lemur bone from southwest Madagascar; the blue and green squares show human presence in northwest Madagascar at 4 ka (human-modified hippopotamus bone) and in northeast Madagascar at 4.4 ka (OSL ages for soil containing microliths), respectively, and the pink squares are ages of human-modified extinct elephant bird bones in southern Madagascar dated to 10.6 and 6.35 ka, respectively. The solid pink and blue settlement lines are speculative as the evidence upon which they are based must be confirmed; the solid red line is considered reliable as it is supported by a variety of solid evidence. The grey bars (labeled M-1 and M-2) define the Crowley (2010) pulses of megafaunal decline. The pink bar defines the most likely timing of the hiatus in sedimentation at Lake Mitsinjo, northwest Madagascar reported by Matsumoto and Burney (1994). AE1 identifies anthropogenic event 1 in Period VI. This occurs at different times in the five stalgmities probably due to age uncertainties; it is only indicated in the ANJ94-5 $\delta^{13}\text{C}$ record. (For interpretation of the references to color in this figure legend, the reader is referred to the Web version of this article.)

Table 3
Correlation of $\delta^{13}\text{C}$ and $\delta^{18}\text{O}$ in five Anjohibe Cave stalagmites during Periods I and VI–VIII.

Periods	Age (ka)	ANJ94-5	AB2	ANJB-2	MA3	MAJ-5
I	9.2–7.5	0.67		0.72		
VI	1.53–0.94	–0.12	–0.11	0.10	–0.07	0.24
VII	0.94–0.34		0.45	0.44	0.60	0.24
VIII	0.34–0.0		0.12	0.18	0.19	–0.15

and/or fewer C_3 plants at Anjokipoty Cave. Values of $\delta^{18}\text{O}$ and $\delta^{13}\text{C}$ for the three Anjohibe Cave stalagmites are positively correlated but relationships are much weaker than during Period VII, suggesting continued human disturbance at the cave. In contrast, $\delta^{18}\text{O}$ and $\delta^{13}\text{C}$ values for MAJ-5 from Anjokipoty Cave are negatively but weakly correlated possibly recording renewed disturbance at the cave after considerable recovery of the natural vegetation during Period VII. At Lake Mitsinjo, the pollen data show a major escalation in disturbance in the last 500 years, evidenced by a highly disturbed grassland with fire-adapted trees and ruderal herbs (Matsumoto and Burney, 1994; Wright et al., 1996). This parallels the evidence from the Anjohibe and Anjokipoty Cave stalagmites of increased human disturbance in Period VII. The changes at Anjohibe Cave were rapid and there is no evidence that the environment around the cave has fully recovered from them.

8. Comparison with regional paleoenvironmental records

8.1. Northern, tropical eastern and southeastern Africa

The African Humid Period (AHP) of northern Africa lasted from ~11.7 to 5 ka (deMenocal et al., 2000; McGee et al., 2013). Many lakes in tropical east Africa were also high during the AHP (Gasse, 2000; Junginger et al., 2014), including Lakes Ziway-Shala (Gillespie et al., 1983) and Turkana (Garcin et al., 2012). Lower leaf wax δD values from Lakes Challa (Tierney et al., 2011a, b) and Tanganyika (Tierney et al., 2008) also suggest wetter conditions in the early Holocene (Fig. 8a–d). The end of the AHP varied across eastern Africa (Costa et al., 2014), but conditions were generally drier after 4 ka. Levels of Lakes Ziway-Shala and Turkana dropped significantly around 5 ka, and leaf wax δD values for Lakes Challa and Tanganyika (Tierney et al., 2008, 2011a) were higher in the last 4 kyr compared to the early Holocene, suggesting drier conditions. Biogenic silica mass accumulation rates in Lake Malawi decreased gradually after 4 ka, suggesting increasingly dry conditions (Johnson et al., 2002).

North Africa was more humid during the AHP (11–5 ka) because increased solar insolation in the Northern Hemisphere during the boreal summer brought the ITCZ further north, raised adjacent ocean SSTs, strengthened monsoons, and enhanced transport of water vapor from oceans to land (e.g. Kutzbach and Otto-Bliesner, 1982). Tropical east Africa and northwest Madagascar were also wet during the AHP, despite both areas being far south of the Equator. Tierney et al. (2011b) refer to the extension of the AHP southward along the east African rift, as the “East African Humid Period” (EAHP). Lakes south of the Equator, such as Lakes Rukwa (8°S) and Cheshi (9°S), had higher water levels (Vincens et al., 2005; Stager, 1988), and lake sediment data for Lakes Tanganyika (6°S) and Victoria (0.8°S) indicate wetter conditions (Tierney et al., 2008; Stager et al., 2003). Gasse (2000) defined latitude 10°S as a “hinge zone” in east Africa in the early-mid Holocene, with wetter conditions to the north and drier to the south. In fact, our evidence from northwest Madagascar indicates that this hinge line bends dramatically to the south off the coast of east Africa and crosses Madagascar somewhere south of 15°S latitude. Therefore, whatever

explanations are offered to explain the EAHP, must also explain synchronous wetter conditions in northwest Madagascar.

Variations in the strength of the East African Monsoon (EAM) indicated by leaf wax δD values from Gulf of Aden core P178-15P (Tierney and deMenocal, 2013) correlate well with evidence in the ANJ94-5 isotope record. When the EAM was strong in the early Holocene, conditions were wet in northwest Madagascar; when the EAM was weak during the last 4 kyr, conditions were drier in northwest Madagascar. In addition, severe droughts evident in the ANJ94-5 data at 4.2 and 4.7 ka correspond with periods of significantly weaker EAM in the Gulf of Aden record (Tierney and deMenocal, 2013). This evidence indicates that EAM strength, driven by Indian Ocean SSTs, may have influenced rainfall in northwest Madagascar during the Holocene.

In the summer rainfall zone of southern Africa, pollen from Wonderkrater indicate arid conditions prior to 7 ka with a trend towards increasing moisture between 7 and 5 ka, moderate moisture levels between 5 and 1 ka, and then much wetter conditions in the last 1 kyr (Fig. 8o; Scott et al., 2003). Pollen from Lake Eteza on the southeast coast of South Africa also suggest drier conditions in the early Holocene prior to 6.8 ka, and humid conditions in the middle Holocene between 6.8 and 3.6 ka (Fig. 8p; Neumann et al., 2010). A particularly dry episode between 8 and 7 ka is indicated at Lake Eteza by very high grass percentages (Neumann et al., 2010). Values of $\delta^{18}\text{O}$ in stalagmites from Cold Air Cave in northeast South Africa also indicate drier conditions in the early Holocene, increasing moisture through the middle Holocene, and generally wet but variable conditions in the late Holocene (Fig. 8n; Lee-Thorp et al., 2001; Holmgren et al., 2003). Zambezi Delta marine sediment core Geob9307-3 δD values of the n-C31 alkane document increasing stream discharge and thus wetter conditions in the Zambezi catchment from the early to late Holocene (Fig. 8m; Schefuß et al., 2011).

Thus, the paleoenvironmental data reveal an antiphase climate relationship between tropical east Africa and southeast Africa, with the former being wetter in the early Holocene and drier in the late Holocene, and the latter drier in the early Holocene and mainly wetter during the late Holocene (Fig. 8, Panels A and C; also Burrough and Thomas, 2013). In fact, measured data show a rainfall dipole with the equatorial east Africa and subtropical southeast Africa poles negatively correlated (Zhang et al., 2015). Importantly, our data from Anjohibe Cave fit with the east African pattern and are opposite to conditions in southeast Africa.

8.2. Madagascar

8.2.1. Environmental records

Tree and grass pollen from stalagmites and cave floor sediments in Anjohibe Cave suggest more wooded savanna during the early and middle Holocene, and an expansion of grassland towards the late Holocene (Burney et al., 1997). Supporting this are $\delta^{13}\text{C}$ data for ^{14}C -dated vertebrate bones from Anjohibe Cave showing that animals in the region consumed negligible C_4 grasses prior to 1 ka, suggesting that the present C_4 -dominated open savanna is relatively recent (Crowley and Samonds, 2013). In addition, as mentioned in Section 7, a 3.5 kyr pollen record from Lake Mitsinjo (Matsumoto and Burney, 1994), shows a hiatus around 1ka that may signify a severe drought and then highly disturbed grassland with fire-adapted trees and ruderal herbs in the last 500 years (Fig. 8f). These findings agree well with the ANJ94-5 record and the other stalagmite records from Anjohibe and Anjokipoty Cave discussed above, and together show that northwest Madagascar was wetter during the early and middle Holocene and drier during the late Holocene and that there was a significant increase in C_4 grasses in the vegetation after ca. 1.5 ka.

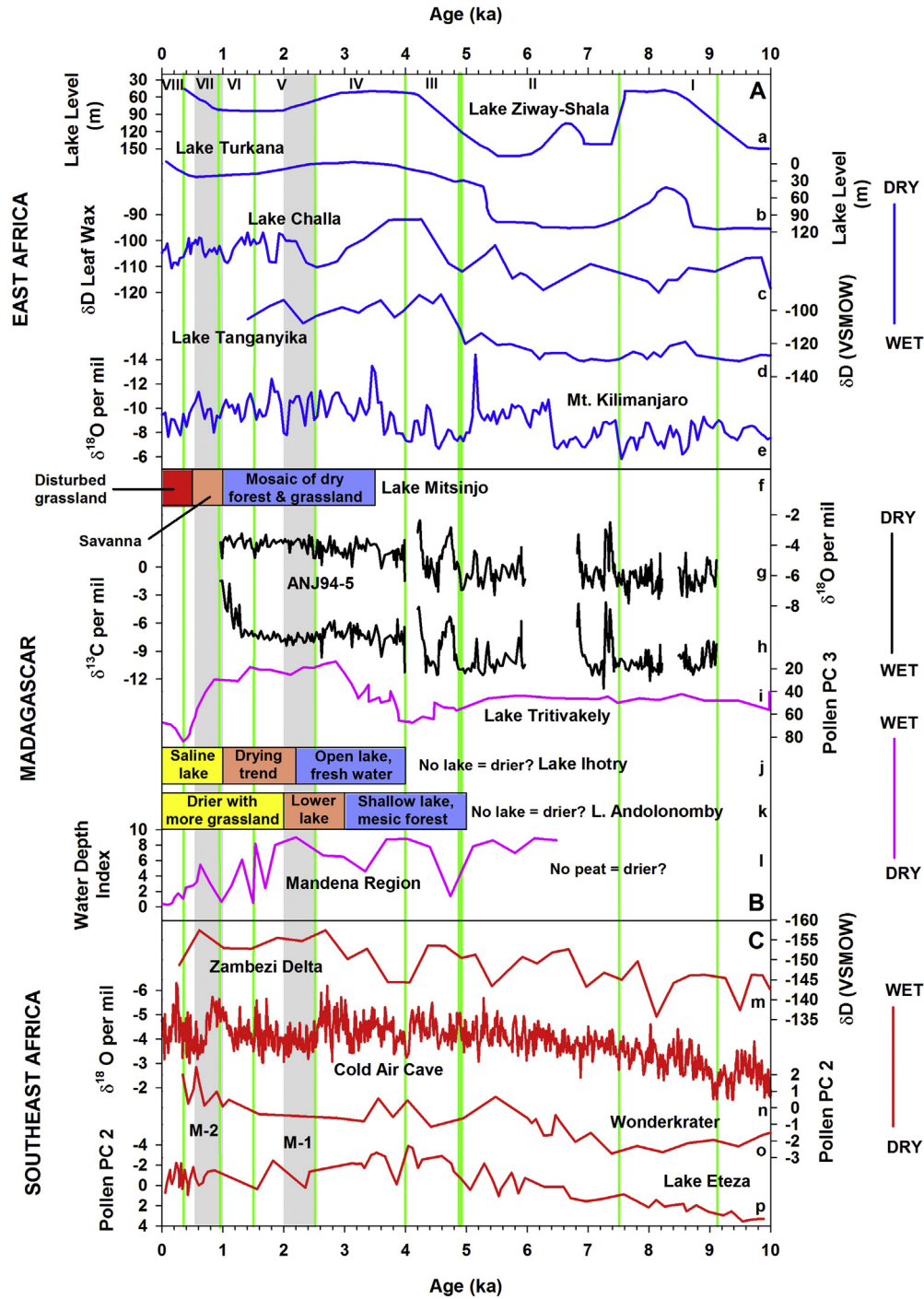


Fig. 8. The ANJ94-5 record compared with other Holocene climate records for Madagascar, east Africa and southeast Africa. East African records in Panel A include: (a) Lake Ziway-Shala (Gillespie et al., 1983); (b) Lake Turkana (Garcin et al., 2012); (c) Lake Challa (Tierney et al., 2011a); (d) Lake Tanganyika (Tierney et al., 2008); and (e) Mt. Kilimanjaro (Thompson et al., 2002). Madagascar records in Panel B include: (f) Lake Mitsinjo (Matsumoto and Burney, 1994); (g and h) oxygen and carbon isotope variations in Stalagmite ANJ94-5 (this paper); (i) Lake Tritivakely pollen principal component P3 (Gasse and Van Campo, 1998); (j) Lake Ihotry (Vallet-Coulomb et al., 2006); (k) Lake Andolononby (Burney, 1993); and (l) diatom-based water depth index from peat depressions in the Mandena region of southeast Madagascar (Virah-Sawmy et al., 2009). Records from southeast Africa in Panel C include: (m) hydrogen isotope variations in the n-31 alkane in marine sediment core GeoB9307-3 from the Zambezi delta (Schefuß et al., 2011); (n) oxygen isotope variations in Stalagmite T8 from Cold Air Cave (Holmgren et al., 2003); (o) principal component 2 of pollen from Wonderkrater (Scott et al., 2003); and (p) Lake Eteza pollen principal component 2 (Neumann et al., 2010). The vertical green lines mark the boundaries of Periods I to VIII (listed at the top of Panel A) with the thick line at 4.9 ka also identifying the end of the African Humid Period. The grey bars (labeled M-1 and M-2) define the Crowley (2010) pulses of megafaunal decline. (For interpretation of the references to color in this figure legend, the reader is referred to the Web version of this article.)

The longest paleoenvironmental records for Madagascar are from sediment cores taken from Lake Tritivakely in the Central Highlands. Mineral-magnetic properties, pollen, total organic carbon, and lithology of the sediments show that the lake was an

ephemeral swamp or oxic basin prior to 6.4 ka and became a permanent swamp-shallow lake afterwards, with the period 3.6–2.2 ka being particularly cool and humid (Williamson et al., 1998). Factor analysis of pollen percentages by Gasse and Van Campo

(1998) indicates drier conditions (increased grass pollen) in the early and middle Holocene with peak dryness around 4 ka, cooler and wetter conditions between 3.8 and 1.6 ka, and much drier conditions after 1 ka, with a significant increase in grass pollen (Fig. 8i). Charcoal studies of a different core at the site recorded high values prior to 4 ka and low values at 3.8–1.2 ka, suggesting more frequent fires in the early and middle Holocene due to drier conditions, and fewer fires during the relatively humid late Holocene prior to human settlement (Burney, 1987a,b,c). These three records agree on Holocene conditions in the Central Highlands, showing drier conditions in the early and middle Holocene and wetter conditions in the late Holocene. This long-term trend in the Central Highlands is opposite to that indicated by the ANJ94-5 data for northwest Madagascar.

Paleoenvironmental records for southern Madagascar are from coastal sites and are often complicated by the effect of sea level changes (e.g., Virah-Sawmy et al., 2009; Vallet-Coulomb et al., 2006). Diatoms and pollen from cores taken from two small (10–20 m diameter) closed peat basins near Mandena on the southeast coast (Fig. 8l) suggest relatively deep water between 6.5 and 2 ka, and more variable but decreasing water depths over the last 2 kyr (Virah-Sawmy et al., 2009). In addition, pollen indicate significant vegetation change after 1.4 ka, with rapid decline of forest and increase of grassland, particularly over the last 950 years (Virah-Sawmy et al., 2009, 2010). In the southwest, the Lake Andolononby basin was formed by fluvial or aeolian processes in the late Pleistocene or early Holocene, probably under relatively dry conditions, but by 5 ka it had become a large shallow lake surrounded by mesic western-Madagascar-type forest suggesting increased rainfall (Fig. 8k). Between 3 and 2 ka a drier climate lowered the lake level and changed the forest to grassland (Burney, 1993). Data from Lake Ihotry in southwest Madagascar (Fig. 8j) show a similar lake history with a transition from drier conditions in the early-middle Holocene (no lake) to a freshwater lake from 4.0 to 2.2 ka, followed by drying and the formation of a closed saline lake around 1 ka (Vallet-Coulomb et al., 2006).

The Central Highland and southern Madagascar paleoenvironmental data show drier conditions in the early-middle Holocene, wetter conditions in the middle-late Holocene, and a much drier climate in the very late Holocene beginning at various times after ca. 3 ka. This parallels changes at sites in southeastern Africa, which show an identical pattern, but is generally opposite to changes in eastern Africa and northwest Madagascar (Fig. 8). This suggests that in broad terms, the climates of the northwest and the central and south regions of the island were antiphase during the Holocene, with the northwest wet (dry) when the central and south were dry (wet).

8.2.2. Human arrival and megafaunal extinctions

In 2010 it appeared that the first megafaunal extinctions in Madagascar had occurred shortly after the arrival of humans around 2.5 ka (Burney et al., 2003, 2004) and this led to the inevitable conclusion that humans were responsible for the demise (Fig. 7). Since then, new evidence has emerged from Anjohibe Cave in northwest Madagascar of cutmarks on *Hippopotamus lemerlei* bones suggesting human butchering at ca. 4 ka (Gommero et al., 2011), and OSL ages of 4.38 ± 0.4 and 3.47 ± 0.37 ka for sediments at the Lakaton'i Anja limestone cave in northeast Madagascar containing microlithic tools (Dewar et al., 2013). Both findings have been challenged; it has been suggested that the cutmarks were produced postmortem during multiple excavations at the Anjohibe site, and that the OSL sediment ages are much older than the microliths they contain because of bioturbation (e.g., Anderson et al., 2018; Hansford et al., 2018). Thus, the view that Madagascar was first colonized around 2.5 ka prevailed.

In 2018, however, Hansford et al. published evidence of human, perimortem cutmarks on bones of elephant birds from southern Madagascar with dates of 10.6 and 6.35 ka. If reliable, the evidence suggests that humans coexisted with megafauna for at least 9 kyr, and that the rapid extinction hypothesis, or blitzkrieg model, for island animal extinctions that has been shown to explain extinctions in for example New Zealand, Hawaii, and Rapa Nui (e.g., Steadman, 1995; Burney, 1997; Burney et al., 1997; Martin and Steadman, 1999; Nunn, 1999; Anderson, 2000; Holdaway and Jacomb, 2000), and which was thought to explain Madagascar extinctions, is not tenable for the island (Hansford et al., 2018). However, before a new paradigm is announced Anderson et al. (2018) urge caution. They stress that more research is needed to confirm the cultural origin of the cutmarks and note that in new excavations they recovered bones >1.1 kyr old from three subfossil sites in southwest Madagascar that had previously provided modified megafaunal bones. These bones showed almost no evidence of typical cultural (human) cutmarks, and instead almost all bone modifications were taphonomic (mechanical or biological). However, cultural cutmarks were much more common on bones of extant taxa dating after ca. 1.2 ka. They argue that previously reported human cutmarks on megafaunal bones from these sites may have been misinterpreted. They conclude that when the paleoecology, genomic and linguistic history, archaeology, introduced biota and seafaring capability are also considered the data they obtained indicate initial human colonization of southwest Madagascar only after 1.35 ka.

If humans were in southern Madagascar at 10.6 ka and 6.35 ka, and in northeast and northwest Madagascar by 4 ka, they left little concrete evidence of their presence. The microliths at Lakaton'i Anja remain of questionable age and none of the bones with possible cutmarks dating to >4 ka is associated with human artifacts (Gommero et al., 2011; Dewar et al., 2013; Hansford et al., 2018). The absence of lithic tools or other human artifacts or remains at the supposed oldest butchering sites in southern Madagascar has led some to suggest that the cutmarks, if genuine, were produced by a small group of humans who stayed only briefly on the island, or stayed but did not survive. In either case they would have had little impact on the island's fauna (e.g., Hansford et al., 2018; Lawler, 2018). Gommero et al. (2011) suggest that “the first populations of humans, comprising a few individuals, probably had a weak environmental impact” (p. 273). The southern interior location of one of these sites (Christmas River) argues against the first of these possibilities but clearly more evidence is needed to confirm the human, perimortem nature of the cut marks given their potential significance.

The ANJ94-5 stalagmite record covers almost all of the Holocene and so it could contain evidence of humans in northwest Madagascar as early as 9.1 ka (Fig. 7). The strong positive correlations between $\delta^{18}\text{O}$ and $\delta^{13}\text{C}$ of stalagmite carbonate during Periods I to III of the record ($r = 0.7$ to 0.9 ; 9.1–4.0 ka) suggest that if humans were present as early as 10.6 ka (Hansford et al., 2018) they did not impact the environment above the cave (Tables 2 and 3). Additionally, if humans were present in northeast Madagascar at Lakaton'i Anja and were butchering hippopotami at Anjohibe Cave around 4 ka (Gommero et al., 2011; Dewar et al., 2013), they clearly had no substantial impact on the Anjohibe area because during Period IV, from 4 to 2.5 ka, $\delta^{18}\text{O}$ and $\delta^{13}\text{C}$ were strongly correlated ($r = 0.63$) suggesting a strong natural link between the area's hydrology and vegetation (Table 3). Admittedly, the first humans to settle Madagascar probably came in small numbers (although in 6.6 kyr from 10.6 to 4.0 ka the numbers could have increased substantially), so they may not have affected the megafauna or their habitat for some time; as a result, Anjohibe Cave stalagmites may not have recorded their presence.

However, the stalagmites at Anjohibe Cave did record major changes at the cave, and possible human presence, after 2.5 ka, in the form of a decoupling of $\delta^{18}\text{O}$ and $\delta^{13}\text{C}$ in the ANJ94-5 record during Period V (2.5–1.53 ka; $r = 0.07$) and Period VI (1.53–0.94 ka; $r = -0.12$). The decoupling records a change in the vegetation near Anjohibe Cave most likely due to human activities indicating that humans were in Madagascar at this time (Fig. 7, Table 3). The change occurs during the transition to agriculture between 3–1.5 ka (Dewar et al., 2013), the spread of settlements across Madagascar by about 1.5 ka, and the occupation of most coastal areas by 0.9 ka (Crowley, 2010; Crowther et al., 2016). Carbon isotope data of vertebrate bones from Anjohibe Cave, northwestern Madagascar suggest minimal consumption of C_4 plants by the extinct animals (Crowley and Samonds, 2013) so the extinct megafauna were mostly forest-dependent. Therefore an increase in agriculture and thus a reduction in forest habitat would have accelerated their decline and this might help to explain why there was not a significant decline in Madagascar's megafauna before 2.5 ka (Crowley, 2010).

Crowley (2010) identifies pulses of megafaunal decline, at 2.5–2.0 and 1.0–0.5 ka. The first affected large and very large species in northwest Madagascar, large species in the Central Highlands, and very large species in southwest Madagascar. The number of megafauna in northwest Madagascar continued to drop after 2.0 ka with the decline rate increasing after 1.5 ka. This increase may have been linked to the major drought evident in the Anjohibe and Anjokipoty Cave stalagmite and Lake Mitsinjo records during Period VI from 1.53 to 0.94 ka, and enhanced by human activities. ANJ94-5 $\delta^{13}\text{C}$ values increase rapidly between 1.5 and 1.0 ka and there is a decoupling of the $\delta^{18}\text{O}$ and $\delta^{13}\text{C}$ time series ($r = -0.12$), strong evidence of significantly reduced rainfall coupled with deforestation by humans, both resulting in the replacement of trees by grass.

The first extinction pulse had less impact in southwest Madagascar, possibly because of the antiphase climate relationship between north and south (it was dry in the north but wetter in the south) and the harsh southern climate that Crowley (2010) believes protected large species from predation by humans. However, the second pulse from 1.0 to 0.5 ka rapidly reduced megafaunal populations in the southwest, most likely due to the combined effects of an increased human population and a shift to much drier conditions. In contrast, as the southwest became much drier, the climate in northwest Madagascar during Anjohibe Cave Period VII from 0.94 to 0.34 ka remained relatively wet (Figs. 7 and 8 B).

Overall, the data suggest that greater aridity in northwest Madagascar after 2.5 ka, including the desiccation of Lake Mitsinjo around 1–1.2 ka, may have enhanced the impact of human predation on the megafauna, while losses in southwest Madagascar, where moisture levels remained relatively high, may have been due only to increased human hunting. The climate at Anjohibe Cave after 1.5 ka was perhaps a little drier than that at 2.5 ka but the impact of humans was much greater and clearly led to a further decline in numbers of megafauna. In southwestern Madagascar there was rapid natural drying of climate after 1.0 ka that probably reduced megafaunal habitat leading to reduced numbers of animals that were still being hunted by humans.

The sudden and rapid increase in $\delta^{13}\text{C}$ values in four stalagmites from Anjohibe Cave and one from Anjokipoty Cave during Period VI signifies major changes in land cover above the caves (Fig. 7). These changes were accompanied by an increase in stalagmite $\delta^{18}\text{O}$ values indicating less rainfall, in fact sufficient to bring about the desiccation of Lake Mitsinjo (Matsumoto and Burney, 1994; Wright et al., 1996) about 115 km and 100 km west-southwest of Anjohibe Cave and Anjokipoty Cave, respectively. However, negative correlations between $\delta^{13}\text{C}$ and $\delta^{18}\text{O}$ in three stalagmites and low positive

correlations in the other two suggest that the magnitude of this “stalagmite isotope event” was triggered by a combination of natural climate change and human activities rather than by natural climate change alone. We refer to this change as anthropogenic event 1 (AE1) and in the five stalagmites it varies in timing from 1.6 ka (MAJ-5) to 1.1 ka (AB2). In ANJ94-5 and AB2 it occurs at around 1.0 ka (Fig. 7). During AE1 $\delta^{13}\text{C}$ increased in ANJ94-5 by 6.03‰ in 322 years while $\delta^{18}\text{O}$ went in the opposite direction, decreasing by 1.63‰. This suggests that the event was triggered at least in part by human clearing of C_3 forest allowing C_4 grasses to dominate and was not due to a natural change in rainfall alone. During the natural RCC events at 7.4, 6.9, 4.7, and 4.2 ka $\delta^{13}\text{C}$ increased by a similar amount (6.06‰–7.69‰) over periods of 118–250 years meaning that the changes were more rapid than during AE1 (Supplement S7), and probably also involved a shift from forest to grass but in these cases induced by significantly lower rainfall, as indicated by increases in $\delta^{18}\text{O}$ values of 2.82‰–3.5‰. In contrast, $\delta^{18}\text{O}$ values in ANJ94-5 increased by only 1.6‰ from –4.8‰ at 1.5 ka to –3.2‰ at 1.3 ka during AE1, again suggesting that humans played a role in elevating the changes in $\delta^{13}\text{C}$ (Fig. 7).

These findings from ANJ94-5 indicate that forest may have been replaced by grassland over large areas during major early-mid Holocene drought events but this did not cause megafaunal extinctions. The magnitude of vegetation change at Anjohibe Cave during the dry conditions of Period VI was at least as great as during the early-mid Holocene drought events, but it was not accompanied by a similar major reduction in rainfall and this may have helped some animals to survive. What was different about the Period VI drought was that humans were hunting drought-stressed megafauna and at the same time destroying their natural habitat. However, only after farming populations had expanded across the island, altering the environment and increasing hunting pressure did the megafauna go extinct (e.g., see Lawler, 2018). The megafauna survived the early-mid Holocene drought events, despite greatly reduced rainfall, and a reduction in forest habitat, but they could not survive the added impact of hunting by humans during the drought of Period VI.

In the past, the antiphase climate relationship between northern and southern Madagascar may have helped the island's megafauna to survive, because at no time was the entire island affected by massive natural drought and forest habitat reduction. Period VI was different because there was human destruction of forest across the island, not just in regions affected by drought. It was probably an increased human population clearing forest for agriculture that finally led to widespread megafaunal extinctions.

Prior to 2011 the preponderance of archaeological, paleoecological, linguistic, genomic, and farming evidence (crops and livestock) suggested a date of about 2.5 ka for the first human colonization of Madagascar (for details see e.g., Burney, 1987a, 1987b, 1987c; Perez et al., 2003; Burney et al., 2004; Hansford et al., 2018; Anderson et al., 2018 (particularly their Fig. 1); and references therein). The evidence from Stalagmite ANJ94-5 appears to confirm that humans were in northwest Madagascar by 2.5 ka and that they were modifying the environment sufficiently for the changes to be registered by actively depositing stalagmites. Even though newly published evidence (Hansford et al., 2018) suggests human presence on the island at 10.6 and 6.5 ka and possibly continuously since the earlier date, there is no evidence in the 9.1–0.94 ka stalagmite record of human impact at the cave prior to 2.5 ka. This lack of evidence does not prove that humans were not in northwest Madagascar prior to 2.5 ka, but if they were, even in small numbers, Anjohibe Cave and the surrounding environment would surely have attracted them to the reliable source of fresh water also used by animals, and they would have modified the environment as humans always do when they enter a new area. If the cultural

cutmarks on early Holocene megafaunal bones from southern Madagascar can be confirmed by the presence of lithic tools or other archaeological artifacts, this will suggest that it was only when human populations were large enough in Madagascar, and/or when they transitioned to agriculture and started to destroy animal habitat that their presence resulted in mass extinctions of megafauna. If the human origin of the cutmarks cannot be confirmed, then the data from ANJ94-5 fits perfectly with a ca. 2.5 ka date for the first arrival of humans in Madagascar.

9. Discussion

9.1. Northern Hemisphere RCC events in northwest Madagascar

The ANJ94-5 data suggest that Holocene Northern Hemisphere RCC events affected Madagascar (e.g., Fig. 7). In particular, the 8.2 and 4.2 ka events of Mayewski et al. (2004) and Walker et al. (2012), or at least their equivalent, are well defined, and date to 8.23–8.48 ka and 4.3–4.0 ka in the ANJ94-5 record. The 4.2 ka event is highlighted by a peak in isotope values at 4.2 ka, followed by a Type L surface and growth hiatus (Hiatus 1) of ca. 200 years. Although there was a brief period of wet conditions around 4 ka, the most prominent feature of the 4.2 ka event in northwest Madagascar was the severe drought that started around 4.3 ka (Fig. 7). The 4.7 ka event appears in the record as a sharp increase in dryness beginning at 4.92 ka and peaking at 4.73 ka; it does not appear to have been as dry as the 4.2 ka event, which may explain why there was no hiatus in stalagmite growth. Both events lasted around 300 years and the changes to peak dryness were very rapid. Of these two events, the most important was probably the 4.2 ka event, because it was followed by a permanent change in climate in northwest Madagascar, towards much drier conditions that prevailed for the next ca. 3 kyr. However, the 4.7 ka event was also significant because we believe it was the start of this event that was used by many researchers to mark the end of the AHP. In fact, McGee et al. (2013) re-dated the end of the AHP to 4.9 ± 0.2 ka, which matches the start of the ANJ94-5 event at 4.92 ka. In contrast to the 4.2 and 4.7 ka dry events, the 8.2 ka event in northwest Madagascar was not cold and dry as in the Northern Hemisphere but is associated with two closely-spaced Type E surfaces and a hiatus caused by dissolutional erosion, indicating significantly wet conditions.

The three younger RCC events of Mayewski et al. (2004) at 3.5–2.5, 1.2–1.0, and 0.6–0.15 ka are not as well represented. The 2.5 ka boundary between Periods IV and V at Anjohibe Cave, roughly corresponds with the oldest of these events; it marks a shift to a less variable climate in northwest Madagascar. The 1.0–1.2 ka RCC event coincides with slight decreases in stalagmites ANJ94-5, ANJB-2, MA3, and AB2 $\delta^{18}\text{O}$ values, indicating increased precipitation, while there is no clear evidence for a 0.6–0.15 RCC event in any of the records (Fig. 7). Importantly, in all four stalagmites, any evidence for the late Holocene RCC events of Mayewski et al. (2004), is greatly overshadowed by a massive shift in stalagmite $\delta^{13}\text{C}$ values with dates ranging from 1.5 to 1.1 ka that was most likely triggered by human activities above the cave. However, during the early and middle Holocene there were climate changes in northwest Madagascar that clearly qualify as RCC events, with dates not mentioned by Mayewski et al. (2004). These include a 200-year drought at 7.2–7.4 ka and a major drought at ca. 6.8 ka, which stopped stalagmite growth (Hiatus 2) for 830 years (6.81–5.98 ka), four times as long as Hiatus 1 during the 4.2 ka event. In the 7.4 and 6.8 ka droughts, the transition from moist to dry was extremely rapid, a few decades at 7.4 ka, and less than a century at 6.8 ka.

9.2. Northwest Madagascar, the AHP, and the EAHP

Climate modeling has reproduced the EAHP and confirms our finding that at 4, 6 and 9 ka it extended into northwest Madagascar (e.g., Tierney et al., 2011b; Singarayer and Burrough, 2015; Chevalier et al., 2017). Model results also show that the climates of north and northwest Madagascar were in phase with north and east Africa during the Holocene but antiphase with south central Madagascar and southeast Africa, confirming our ANJ94-5 data. The HadCM3 4, 6, and 9 ka simulations of Singarayer and Burrough (2015) clearly show that the AHP wet period extends along the east African rift valleys into north and northwest Madagascar (Fig. 9). The much drier conditions of south central Madagascar and southeast Africa are also clearly evident. Reduced rainfall anomalies in the Singarayer and Burrough (2015) 4 ka simulation agree with our ANJ94-5 stalagmite data that this was a transition period towards drier conditions in northwest Madagascar.

Simulations by Tierney et al. (2011b), using the GISS ModelE-R, differ from those of Singarayer and Burrough (2015), in that they document anomalies in P-E rather than just P. However, their simulation of annual P-E anomalies for 6 ka shows increased moisture in north and northwest Madagascar and an extension of wet conditions southward along the rift valley system. Tierney et al. (2011b) suggest that the most important factor contributing to the EAHP was a change in dry season (Jun–Nov) precipitation and reduced precipitation seasonality, with moisture in east Africa coming from both the Atlantic and Indian Oceans. Tierney et al. (2011b) also found reduced precipitation from Dec–May in both east and southern Africa in their simulation, which they believe was probably caused by the cooling of the continent during the boreal winter and an increase in offshore transfer of precipitation, not by a shift in the ITCZ over land. Areas south of 10°S are generally drier in the 6 ka simulation, consistent with the “hinge zone” of Gasse (2000), probably due to the large reduction in December–March precipitation caused by continental cooling, rather than a mean northward shift in the position of the ITCZ.

10. Conclusions

Multiproxy climate data from ANJ94-5, and other published stalagmite data for northwest Madagascar, suggest the following conclusions:

- i) There were six distinct Holocene climate/environment periods in northwest Madagascar from 9.1 to 0.94 ka based on the ANJ94-5 records. Period I (9.1–7.5 ka) was the wettest of the entire ANJ94-5 record, with little climate variability and vegetation dominated by C_3 trees. Conditions were extremely wet at ca. 8.2 ka when undersaturated dripwater removed ca. 260 years of previously deposited carbonate (Hiatus 3); this interval may correlate with the 8.2 ka cold event of the Northern Hemisphere.
- ii) The climate during Period II (7.5–4.9 ka) varied greatly between intervals of wetness and a series of significant droughts, each lasting 100–300 years. The significant drought at ca. 6.9 ka resulted in a hiatus (Hiatus 2) in stalagmite growth due to a lack of dripwater.
- iii) Period III (4.9–4 ka) was a time of transition from relatively wet and variable climate to much drier and less variable climate. It is marked by two prominent dry intervals at ca. 4.7 ka and 4.2 ka, the second of which may be the expression of the global 4.2 ka climate event in northwest Madagascar.
- iv) Climate was less variable beginning with Period IV (4–2.5 ka) and the shift to overall drier conditions after ca. 4 ka was permanent with dryness increasing steadily to 2.6 ka.

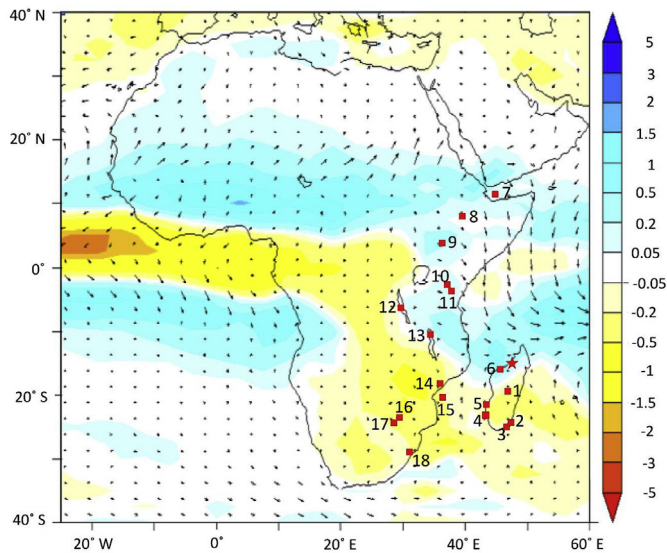


Fig. 9. HadCM3 simulation of annual mean precipitation anomalies and 10m wind anomalies for MH-PI for 6 ka showing sites mentioned in the text (see Supplement S2 for details). Figure is modified from Fig. S7 of Singarayer and Burroughs (2015). Wet conditions in north and east Africa, the east African rift valleys, and northwest Madagascar during the AHP and EAHP are clearly visible. Details of Sites 1–18 and the proxy climate data they have provided are given in Supplement S2.

Conditions remained dry with little variability throughout Periods V (2.5–1.53 ka) and VI (1.53–0.94 ka). Vegetation was probably a mix of trees and grasses during Periods IV and V, possibly a palm savanna as today, but C_4 grasses increased significantly during Period VI.

- v) Based on published data for five other stalagmites from the area, it appears that there were two additional climate periods after ANJ94-5 stopped growing. Period VII (0.94–0.34 ka) was dry overall with a more stable grassy vegetation cover at Anjohibe Cave but a change back to a C_3 dominated vegetation at Anjokipoty Cave, indicating continued human disturbance at Anjohibe but an end to human disturbance at Anjokipoty with a reversion to the “natural vegetation”. Period VIII (0.34–0 ka) saw a slight increase in rainfall in northwest Madagascar and continued human disturbance of the environment.
- vi) The carbon and oxygen isotope records are positively and strongly correlated during Periods I to IV but the correlation weakens in Period V ($r = 0.07$) and Period VI ($r = -0.12$). The decoupling of the carbon and oxygen isotope values at Anjohibe Cave might signal human impact on the landscape, beginning around 2.5 ka, and supporting other evidence for human presence in northwest Madagascar in sufficient numbers to impact the environment.
- vii) ANJ94-5 wet Periods I and II, and dry Periods IV–VI, are antiphase with the Central Highlands and the southern regions of Madagascar, where these periods were dry and wet, respectively.
- viii) The Northern Hemisphere 8.2 and 4.2 ka RCC events are well defined in the ANJ94-5 record and there is also evidence of a 5.2 ka event. The 8.2 ka event was wet, unlike its Northern Hemisphere counterpart, which was cold and dry. The other two events were marked by significant droughts in northwest Madagascar.
- ix) Madagascar’s megafauna survived a number of severe droughts in the northwest region during the early-mid Holocene, suggesting that droughts were not in themselves

responsible for late Holocene megafaunal extinctions. Instead, the evidence suggests that megafaunal populations, possibly reduced in numbers by increasingly dry natural conditions across the island after ca. 4 ka, were severely impacted by human activities, particularly hunting and habitat destruction related to the transition from foraging to agriculture.

- x) Despite being 15° south of the Equator, climate changes in northwest Madagascar parallel AHP changes in north Africa and EAHP changes in tropical east Africa but are antiphase with conditions in south central Madagascar and southeast Africa. This means that the climate near Anjohibe Cave is not determined exclusively by the location of the ITCZ in austral summer.

Acknowledgments

This research was supported by NOAA grant NA56GP0325 (Brook, Railsback, Thill and Meltzer), NSF grants 8912046 (Brook, Burney and Cowart) and 9908415 (Brook and Railsback), and NSFC grant 41888101 (Cheng). We thank the government and people of Madagascar for their assistance in making this work possible. Fieldwork in Madagascar was carried out under the auspices of the Cenozoic Research Group, a Malagasy-American collaboration sanctioned by the Service de Paléontologie and the Musée d’Art et d’Archéologie of the Université d’Antananarivo.

Appendix A. Supplementary data

Supplementary data to this article can be found online at <https://doi.org/10.1016/j.quascirev.2019.02.004>.

References

- Anderson, A.J., 2000. Defining the period of moa extinction. *Archaeol. N. Z.* 43, 195–200.
- Anderson, A., Clark, G., Haberle, S., Higham, T., Nowak-Kemp, M., Prendergast, A., Radimilaha, C., Rakotozafy, L.M., Ramilisonina, Schwenninger, J.-L., Virah-Sawmy, M., Camens, A., 2018. New evidence of megafaunal bone damage indicates late colonization of Madagascar. *PLoS One* 13 (10), e0204368. <https://doi.org/10.1371/journal.pone.0204368>.
- Brook, G.A., Rafter, M.A., Railsback, L.B., Sheen, S.-W., Lundberg, J., 1999. A high-resolution proxy record of rainfall and ENSO since A.D. 1550 from layering in stalagmites from Anjohibe Cave, Madagascar. *Holocene* 9 (6), 695–705.
- Burgess, N., Hales, J.D., Underwood, E., Dinerstein, E., Olson, D., Itoua, I., Newman, K., 2004. Terrestrial ecoregions of Africa and Madagascar: a conservation assessment. In: Burgess, N., Hales, J.A., Underwood, E., Dinerstein, E. (Eds.), *Terrestrial Ecoregions of Africa and Madagascar: a Conservation Assessment*. Island Press, Washington; USA.
- Burney, D.A., 1987a. Pre-settlement vegetation changes at Lake Tritrivakely, Madagascar. *Palaeoecol. Afr.* 18, 357–381.
- Burney, D.A., 1987b. Late Quaternary stratigraphic charcoal records from Madagascar. *Quat. Res.* 28, 274–280.
- Burney, D.A., 1987c. Late Holocene vegetational change in central Madagascar. *Quat. Res.* 28 (1), 130–143.
- Burney, D.A., 1993. Late Holocene environmental changes in arid southwestern Madagascar. *Quat. Res.* 40 (1), 98–106.
- Burney, D.A., 1997. Tropical islands as paleoecological laboratories: gauging the consequences of human arrival. *Hum. Ecol.* 25 (3), 437–457.
- Burney, D.A., Ramilisonina, Wright, H.T., Cowart, J.B., James, H.F., Grady, F.V., Rafamantanantsoa, J.G., 1997. Environmental change, extinction and human activity: evidence from caves in northwest Madagascar. *J. Biogeogr.* 24 (6), 755–767.
- Burney, D.A., Robinson, G.S., Burney, L.P., 2003. *Sporormiella* and the late Holocene extinctions in Madagascar. *Proc. Natl. Acad. Sci., U.S.A.* 100, 10800–10805.
- Burney, D.A., Burney, L.P., Godfrey, L.R., Jungers, W.L., Goodman, S.M., Wright, H.T., Jull, A.J.T., 2004. A chronology for late prehistoric Madagascar. *J. Hum. Evol.* 47, 25–63.
- Burns, S.J., Godfrey, L.R., Faina, P., McGee, D., Hardt, B., Ranivoharimanana, L., Randrianasy, J., 2016. Rapid human-induced landscape transformation in Madagascar at the end of the first millennium of the Common Era. *Quat. Sci. Rev.* 134, 92–99.
- Burroughs, S.L., Thomas, D.S.G., 2013. Central southern Africa at the time of the African Humid Period; a new analysis of Holocene palaeoenvironmental and

- palaeoclimate data. *Quat. Sci. Rev.* 80, 29–46.
- Cheng, H., Fleitmann, D., Edwards, R.L., Wang, X., Cruz, F.W., Auler, A.S., Mangini, A., Wang, Y., Kong, X., Burns, S., Matter, A., 2009. Timing and structure of the 8.2 kyr B.P. event inferred from delta ¹⁸O records of stalagmites from China, Oman, and Brazil. *Geology* 37 (11), 1007–1010.
- Chevalier, M., Brewer, S., Chase, B.M., 2017. Qualitative assessment of PMIP3 rainfall simulations across the eastern African monsoon domains during the mid-Holocene and the Last Glacial Maximum. *Quat. Sci. Rev.* 156, 107–120.
- Costa, K., Russell, J., Konecky, B., Lamb, H., 2014. Isotopic reconstruction of the African Humid Period and Congo Air Boundary migration at Lake Tana, Ethiopia. *Quat. Sci. Rev.* 83, 58–67.
- Crowley, B.E., 2010. A refined chronology of prehistoric Madagascar and the demise of the megafauna. *Quat. Sci. Rev.* 29, 2591–2603.
- Crowley, B.E., Samonds, K.E., 2013. Stable carbon isotope values confirm a recent increase in grasslands in northwestern Madagascar. *Holocene* 23 (7), 1066–1073.
- Crowther, A., Lucas, L., Helm, R., Horton, M., Shipton, C., Wright, H.T., Walshaw, S., Pawlowicz, M., Radimilay, C., Douka, K., Picornell-Gelabert, L., Fuller, D.Q., Boivin, N.L., 2016. Ancient crops provide first archaeological signature of the westward Austronesian expansion. *Proc. Natl. Acad. Sci. U.S.A.* 113, 6635–6640.
- de Menocal, P., Ortiz, J., Guilderson, T., Adkins, J., Sarnthein, M., Baker, L., Yarusinsky, M., 2000. Abrupt onset and termination of the African Humid Period: rapid climate responses to gradual insolation forcing. *Quaternary Science Reviews* 19 (15), 347–361.
- Dewar, R.E., Radimilay, C., Wright, H.T., Jacobs, Z., Kelly, G.O., Berna, F., 2013. Stone tools and foraging in northern Madagascar challenge Holocene extinction models. *Proc. Natl. Acad. Sci.* 110 (31), 12583–12588.
- Fairchild, I.J., Smith, C.L., Baker, A., Fuller, L., Spötl, C., Matthey, D., McDermott, F., E.I.M.F., 2006. Modification and preservation of environmental signals in speleothems. *Earth Science Reviews* 75, 105–153.
- FEWS NET (Famine Early Warning Systems Network), 2014. SOUTHERN AFRICA Special Report: 2014/15 El Niño Event. USAID, p. 2. www.fews.net/South.
- Frumkin, A., Ford, D.C., Schwarcz, H.P., 2000. Paleoclimate and vegetation of the last glacial cycles in Jerusalem from a speleothem record. *Glob. Biogeochem. Cycles* 14, 863–870.
- Garcin, Y., Melnick, D., Strecker, M.R., Olago, D., Tiercelin, J.J., 2012. East African mid-Holocene wet–dry transition recorded in palaeo-shorelines of Lake Turkana, northern Kenya Rift. *Earth Planet. Sci. Lett.* 331, 322–334.
- Gasse, F., 2000. Hydrological changes in the African tropics since the Last Glacial Maximum. *Quat. Sci. Rev.* 19, 189–211.
- Gasse, F., Van Campo, E., 1998. A 40,000-yr pollen and diatom record from Lake Tritrivakely, Madagascar, in the southern tropics. *Quat. Res.* 46, 299–311.
- Gillespie, R., Street-Perrott, F.A., Switsur, R., 1983. Post-glacial arid episodes in Ethiopia have implications for climate prediction. *Nature* 306, 680–683.
- Gommery, D., Ramanivosoa, B., Faure, M., Guérin, C., Kerloch, P., Sénégas, F., Randrianantenaina, H., 2011. Les plus anciennes traces d'activités anthropiques de Madagascar sur des ossements d'hippopotames fossiles d'Anjohibe (Province de Mahajanga). *Comptes Rendus Palevol* 10, 271–278.
- Hansford, J., Wright, P.C., Rasoamiamanana, A., Pérez, V.R., Godfrey, L.R., Errickson, D., Thompson, T., Turvey, S.T., 2018. Early Holocene human presence in Madagascar evidenced by exploitation of avian megafauna. *Sci. Adv.* 4, eaat6925.
- Holdaway, R.N., Jacomb, C., 2000. Rapid extinction of the moas (*Aves*: Dinornithiformes): model, test, and implications. *Science* 287, 2250–2254.
- Holmgren, K., Lee-Thorp, J.A., Cooper, G.R.J., Lundblad, K., Partridge, T.C., Scott, L., Sthaldeen, R., Talma, A.S., Tyson, P.D., 2003. Persistent millennial-scale climatic variability over the past 25,000 years in Southern Africa. *Quat. Sci. Rev.* 22 (21–22), 2311–2326.
- Ingram, J.C., Dawson, T.P., 2005. Climate change impacts and vegetation response on the island of Madagascar. *Phil. Trans. Roy. Soc. London Series a-Math. Phys. Eng. Sci.* 363 (1826), 55–59.
- Junginger, A., Roller, S., Olaka, L.A., Trauth, M.H., 2014. The effects of solar irradiation changes on the migration of the Congo Air Boundary and water levels of paleo-Lake Suguta, Northern Kenya Rift, during the African Humid Period (15–5 ka BP). *Palaeogeogr. Palaeoclimatol. Palaeoecol.* 396, 1–16.
- Johnson, T.C., Brown, E.T., McManus, J., Barry, S., Barker, P., Gasse, F., 2002. A high-resolution paleoclimate record spanning the past 25,000 years in southern East Africa. *Science* 296 (5565), 113–132.
- Jury, M.R., Nasser, A., Parker, B.A., Raholjao, N., 1995. Variability of summer rainfall over Madagascar: climatic determinants at interannual scales. *Int. J. Climatol.* 15 (12), 1323.
- Jury, M.R., 2003. The climate of Madagascar. In: Goodman, S.M., Benstead, J.P. (Eds.), *The Natural History of Madagascar*. The University of Chicago Press, pp. 75–87.
- Kim, S.T., O'Neil, J.R., Hillaire-Marcel, C., Mucci, A., 2007. Oxygen isotope fractionation between synthetic aragonite and water: influence of temperature and Mg²⁺ concentration. *Geochim. Cosmochim. Acta* 71, 4704–4715.
- Kreppel, K.S., Caminade, C., Telfer, S., Rajerison, M., Rahalison, L., Morse, A., Baylis, M., 2014. A non-stationary relationship between global climate phenomena and human plague incidence in Madagascar. *PLoS Negl. Trop. Dis.* 8 (10), e3155. <https://doi.org/10.1371/journal.pntd.0003155>.
- Kutzbach, J.E., Otto-Bliesner, B.L., 1982. The sensitivity of the African–Asian monsoonal climate to orbital parameter changes for 9000 years BP in a low-resolution general circulation model. *J. Atmos. Sci.* 39, 1177–1188.
- Lachniet, M.S., 2009. Climatic and environmental controls on speleothem oxygen isotope values. *Quaternary Science Reviews* 28, 412–432.
- Lawler, A., 2018. Scarred bird bones reveal early settlement on Madagascar. *Science* 361 (6407), 1059.
- Lee-Thorp, J.A., Holmgren, K., Lauritzen, S.E., Linge, H., Moberg, A., Partridge, T.C., Stevenson, C., Tyson, P.D., 2001. Rapid climate shifts in the southern African interior throughout the mid to late Holocene. *Geophys. Res. Lett.* 28 (23), 4507–4510.
- Martin, P.S., Steadman, D.W., 1999. Prehistoric extinctions on islands and continents. In: MacPhee, R.D.E. (Ed.), *Extinctions in Near Time*. Kluwer Academic/Plenum, New York, pp. 17–55.
- Mason, S.J., 2001. El Niño, climate change, and Southern African climate. *Environmetrics* 12, 327–345.
- Mason, S.J., Jury, M.R., 1997. Climatic variability and change over southern Africa: a reflection on underlying processes. *Prog. Phys. Geogr.* 21 (1), 23–50.
- Matsumoto, K., Burney, D.A., 1994. Late Holocene environments at Lake Mitsinjo, northwestern Madagascar. *Holocene* 4 (1), 16–24.
- Mayewski, P.A., Rohling, E.E., Stager, C.J., Karlen, W., Maasch, K.A., Meeker, L.D., Meyerson, E.A., Gasse, F., van Kreveld, S., Holmgren, K., Lee-Thorp, J., Rosqvist, G., Rack, F., Staubwasser, M., Schneider, R.R., Steig, E.J., 2004. Holocene climate variability. *Quat. Res.* 62 (3), 243–255.
- McDermott, F., 2004. Palaeo-climate reconstruction from stable isotope variations in speleothems: a review. *Quaternary Science Reviews* 23, 901–918.
- McGee, D., deMenocal, P.B., Winckler, G., Stuetz, J.B.W., Bradtmiller, L.I., 2013. The magnitude, timing and abruptness of changes in North African dust deposition over the last 20,000 yr. *Earth and Planetary Science Letters* 371–372, 163–176.
- Middleton, J., Middleton, V., 2002. Karst and caves of Madagascar. *Cave Karst Sci.* 29, 13–20.
- Mickler, P.J., Stern, L.A., Banner, J.L., 2006. Large kinetic isotope effects in modern speleothems. *Geol. Soc. Am. Bull.* 118, 65–81.
- Neukom, R., Nash, D.J., Endfield, G.H., Grab, S.W., Grove, C.A., Kelso, C., Vogel, C.H., Zinke, J., 2014. Multi-proxy summer and winter precipitation reconstruction for southern Africa over the last 200 years. *Clim. Dyn.* 42, 2713–2726. <https://doi.org/10.1007/s00382-013-1886-6>.
- Neumann, F.H., Scott, L., Bousman, C.B., van As, L., 2010. A Holocene sequence of vegetation change at Lake Eteza, coastal KwaZulu-Natal, South Africa. *Rev. Palaeobot. Palynol.* 162, 39–53.
- Nunn, P.D., 1999. Environmental catastrophe in the Pacific islands around A.D. 1300. *Geoarchaeology* 15, 715–740.
- Overpeck, J.T., 1996. Warm climate surprises. *Science* 271, 1820–1821.
- Perez, V.R., Burney, D.A., Godfrey, L.R., Nowak-Kemp, M., 2003. Butchered sloth lemurs. *Evol. Anthropol.* 12, 260.
- Railsback, L.B., Akers, P.D., Wang, L., Holdridge, G.A., Voarintsoa, N.R., 2013. Layer-bounding surfaces in stalagmites as keys to better paleoclimatological histories and chronologies. *Int. J. Speleol.* 42 (3), 167–180.
- Railsback, L.B., Brook, G.A., Webster, J.W., 1999. Petrology and paleoenvironmental significance of detrital sand and silt in a stalagmite from Drotzky's Cave, Botswana. *Physical Geography* 20 (4), 331–347.
- Reason, C.J.C., Rouault, M., 2002. ENSO-like decadal variability and South African rainfall. *Geophys. Res. Lett.* 29 (10), 1029.
- Romanek, C.S., Grossman, E.E., Morse, J.W., 1992. Carbon isotopic fractionation in synthetic aragonite and calcite: effects of temperature and precipitation rate. *Geochim. Cosmochim. Acta* 56, 419–430.
- Ropelewski, C.F., Halpert, M.S., 1987. Global and regional scale precipitation patterns associated with the El Niño/Southern Oscillation. *Mon. Weather Rev.* 115 (8), 1606–1626.
- Ropelewski, C.F., Halpert, M.S., 1989. Precipitation patterns associated with the high index phase of the Southern Oscillation. *J. Clim.* 2, 268–284.
- Schefuß, E., Kuhlmann, H., Mollenhauer, G., Prange, M., Paetzold, J., 2011. Forcing of wet phases in southeast Africa over the past 17,000 years. *Nature* 480 (7378), 509–512.
- Scholz, D., Hoffmann, D.L., 2011. Research Paper: StalAge – an algorithm designed for construction of speleothem age models. *Quat. Geochronol.* 6, 369–382.
- Scott, L., Holmgren, K., Talma, A.S., Woodborne, S., Vogel, J.C., 2003. Age interpretation of the Wonderkrater spring sediments and vegetation change in the Savanna Biome, Limpopo Province, South Africa. *South Afr. J. Sci.* 99 (9), 484–494.
- Scroxton, N., Burns, S.J., McGee, D., Hardt, B., Godfrey, L.R., Ranivoharimanana, L., Faina, P., 2017. Hemispherically in-phase precipitation variability over the last 1700 years in a Madagascar speleothem record. *Quat. Sci. Rev.* 164, 25–36.
- Singarayer, J.S., Burrough, S.L., 2015. Interhemispheric dynamics of the African rainbelt during the late Quaternary. *Quat. Sci. Rev.* 124, 48–67.
- Sletten, H.R., Railsback, L.B., Liang, F., Brook, G.A., Marais, E., Hardt, B.F., Edwards, R.L., 2013. A petrographic and geochemical record of climate change over the last 4600 years from a northern Namibia stalagmite, with evidence of abruptly wetter climate at the beginning of southern Africa's Iron Age. *Palaeogeogr. Palaeoclimatol. Palaeoecol.* 376, 149–162.
- Stager, J.C., 1988. Environmental changes at Lake Cheshi, Zambia since 40,000 years B.P. *Quat. Res.* 29, 54–65.
- Stager, J.C., Cumming, B.F., Meeker, L.D., 2003. A 10,000-year high-resolution diatom record from Pilkington Bay, Lake Victoria, East Africa. *Quat. Res.* 59, 172–181.
- Steadman, D.W., 1995. Prehistoric extinctions of Pacific island birds: biodiversity meets zooarchaeology. *Science* 267, 1123–1131.
- Tadross, M., Randriamarolaza, L., Rabefitia, Z., Zheng, K.Y., 2008. Climate Change in Madagascar; Recent Past and Future. World Bank, Washington, DC, p. 18.
- Thompson, L.G., Mosley-Thompson, E., Davis, M.E., Hendersen, K.A., Brecher, H.H., Zagorodnov, V.S., Beer, J., 2002. Kilimanjaro Ice Core Records: Evidence of

- Holocene Climate Change in Tropical Africa. *Science* 298 (5593), 589–593.
- Tierney, J.E., deMenocal, P.B., 2013. Abrupt Shifts in Horn of Africa Hydroclimate Since the Last Glacial Maximum. *Science* 342 (6160), 843–846.
- Tierney, J.E., Russell, J.M., Huang, Y., Damsté, J.S.S., Hoppmans, E.C., Cohen, A.S., 2008. Northern Hemisphere Controls on Tropical Southeast African Climate During the Past 60,000 Years. *Science* 322 (5899), 252–255.
- Tierney, J.E., Russell, J.M., Sinninghe Damsté, J.S., Huang, Y., Verschuren, D., 2011a. Late Quaternary behavior of the East African monsoon and the importance of the Congo Air Boundary. *Quat. Sci. Rev.* 30, 798–807.
- Tierney, J.E., Lewis, S.C., Cook, B.I., LeGrande, A.N., Schmidt, G.A., 2011b. Model, proxy and isotopic perspectives on the East African Humid Period. *Earth Planet. Sci. Lett.* 307, 103–112.
- Vallet-Coulomb, C., Gasse, F., Robison, L., Ferry, L., Van Campo, E., Chalie, F., 2006. Hydrological modeling of tropical closed Lake Ihotry (SW Madagascar): sensitivity analysis and implications for paleohydrological reconstructions over the past 4000 years. *J. Hydrol.* 331 (1–2), 257–271.
- Vincens, A., Buchet, G., Williamson, D., Taieb, M., 2005. A 23,000 yr pollen record from Lake Rukwa (8°S, SW Tanzania): new data on vegetation dynamics and climate in Central Eastern Africa. *Rev. Palaeobot. Palynol.* 137, 147–162.
- Virah-Sawmy, M., Willis, K.J., Gillson, L., 2009. Threshold response of Madagascar's littoral forest to sea-level rise. *Glob. Ecol. Biogeogr.* 18 (1), 98–110.
- Virah-Sawmy, M., Willis, K.J., Gillson, L., 2010. Evidence for drought and forest declines during the recent megafaunal extinctions in Madagascar. *J. Biogeogr.* 37 (3), 506–519.
- Voarintsoa, N.R.G., Wang, L., Railsback, L.B., Brook, G.A., Liang, F., Cheng, H., Edwards, R.L., 2017a. Multiple proxy analyses of a well-dated and well-replicated stalagmite to reconstruct paleoenvironmental changes in north-western Madagascar between AD 370 and AD 1300. *Palaeogeogr. Palaeoclimatol. Palaeoecol.* 469, 138–155.
- Voarintsoa, N.R.G., Railsback, L.B., Brook, G.A., Wang, L., Kathayat, G., Cheng, H., Li, X., Edwards, R.L., Michel, R.A.F., Olga, M.R.F., 2017b. Three distinct Holocene intervals revealed in northwest Madagascar: evidence from two stalagmites from two caves, and implications for ITCZ dynamics. *Clim. Past* 13, 1771–1790. <https://doi.org/10.5194/cp-13-1771-2017>.
- Voarintsoa, N.R.G., Matero, I.S.O., Railsback, L.B., Gregoire, L.J., Tindall, J., Sime, L., Cheng, H., Edwards, R.L., Brook, G.A., Kathayat, G., Li, X., Rakotondrazafy, A.F.M., Razanantseho, M.O.M., 2019. Investigating the 8.2 ka event in northwestern Madagascar: insight from data-model comparisons. *Quat. Sci. Rev.* 204, 172–186.
- Walker, M.J.C., Berkelhammer, M., Björck, S., Cwynar, L.C., Fisher, D.A., Long, A.J., Lowe, J.J., Newnham, R.M., Rasmussen, S.O., Weiss, H., 2012. Formal subdivision of the Holocene Series/Epoch: a Discussion Paper by a Working Group of INTIMATE (Integration of ice-core, marine and terrestrial records) and the Subcommission on Quaternary Stratigraphy (International Commission on Stratigraphy). *J. Quat. Sci.* 27, 649–659.
- Webster, J.W., Brook, G.A., Railsback, L.B., Cheng, H., Edwards, R.L., Alexander, C., Reeder, P.P., 2007. Stalagmite evidence from Belize indicating significant droughts at the time of preclassic abandonment, the Maya hiatus, and the classic Maya collapse. *Palaeogeogr. Palaeoclimatol. Palaeoecol.* 250, 1–17.
- Williamson, D., Jelinowska, A., Kissel, C., Tucholka, P., Gibert, E., Gasse, F., Wieckowski, K., 1998. Mineral-magnetic proxies of erosion/oxidation cycles in tropical maar-lake sediments (Lake Tritrivakely, Madagascar): paleoenvironmental implications. *Earth Planet. Sci. Lett.* 155 (3–4), 205–219.
- Wright, H.T., Vêrin, P., Ramilisonina, Burney, D., Burney, L.P., Matsumoto, K., 1996. The evolution of settlement systems in the Bay of Boeny and the Mahavavy River valley, north-western Madagascar. *Azania* 32, 37–73.
- Zhang, Q., Holmgren, K., Sundqvist, H., 2015. Decadal Rainfall Dipole Oscillation over Southern Africa Modulated by Variation of Austral Summer Land–Sea Contrast along the East Coast of Africa. *J. Atmos. Sci.* 72 (5), 1827–1836.
- Zinke, J., Dullo, W.C., Heiss, G.A., Eisenhauer, A., 2004. ENSO and Indian Ocean subtropical dipole variability is recorded in a coral record off southwest Madagascar for the period 1695 to 1995. *Earth Planet. Sci. Lett.* 228 (1–2), 177–194.